
Scalable Bayesian Monte Carlo: fast uncertainty estimation beyond deep ensembles

Xinzhu Liang

Mathematics Department, University of Manchester
Manchester, M13 9PL, UK
xinzhu.liang@postgrad.manchester.ac.uk

Joseph M. Lukens*

School of Electrical and Computer Engineering
Purdue University, West Lafayette, Indiana 47907, USA

Sanjaya Lohani

Department of Electrical and Computer Engineering,
Southern Methodist University, Dallas, Texas 75205, USA

Brian T. Kirby†

DEVCOM US Army Research Laboratory
Adelphi, Maryland 20783, USA

Thomas A. Searles

Department of Electrical and Computer Engineering,
University of Illinois Chicago, Chicago, Illinois 60607, USA

Xin Qiu

Cognizant AI Labs
San Francisco, California 94105, USA

Kody J. H. Law‡

Mathematics Department, University of Manchester
Manchester, M13 9PL, United Kingdom

Abstract

This work introduces a *new method* designed for Bayesian deep learning called scalable Bayesian Monte Carlo (SBMC). The method is comprised of a *model* and an *algorithm*. The model interpolates between a point estimator and the posterior. The algorithm is a *parallel* implementation of sequential Monte Carlo sampler (SMC_{||}) or Markov chain Monte Carlo (MCMC_{||}). We collectively refer to these *consistent* (asymptotically unbiased) algorithms as *Bayesian Monte Carlo* (BMC), and any such algorithm can be used in our SBMC method. The utility of the method is demonstrated on practical examples: MNIST, CIFAR, IMDb. A systematic numerical study reveals that *for the same wall-clock time as state-of-the-art (SOTA) methods like deep ensembles (DE)*, SBMC achieves comparable or better accuracy and substantially improved uncertainty quantification (UQ)–*in particular, epistemic UQ*. This is demonstrated on the downstream task of estimating the confidence in predictions, which can be used for reliability assessment or abstention decisions.

*Quantum Information Science Section, Oak Ridge National Laboratory, Oak Ridge, Tennessee 37831, USA

†Tulane University, New Orleans, Louisiana 70118, USA

‡KLAI Ltd, London, EC1V 2NX, UK, and Amadeus Protocol, Toronto, ON, M5C 1C4, CA.

1 Introduction

Uncertainty quantification (UQ) in deep learning is critical for safe and reliable deployment, yet remains a core challenge. The Bayesian formulation provides UQ in addition to Bayes optimal accuracy, by averaging realizations from the posterior distribution, rather than relying on a single point estimator. Fully Bayesian approaches like consistent Markov chain Monte Carlo (MCMC) and sequential Monte Carlo (SMC) offer asymptotically unbiased posterior estimates, but at the cost of prohibitive compute time compared to simple point estimators like the maximum a posteriori (MAP). Bayesian deep learning (BDL) often rely on scalable approximations such as Monte Carlo Dropout [Gal and Ghahramani, 2016], deep ensemble (DE) [Lakshminarayanan et al., 2017], Laplace approximation [Daxberger et al., 2021, Eschenhagen et al., 2021], Stochastic Weight Averaging (SWA) [Izmailov et al., 2018], SWA-Gaussian (SWAG) [Maddox et al., 2019, Wilson and Izmailov, 2020], which are fast and provide strong empirical performance, but lack formal consistency guarantees.

Here we present a new approximate inference method called Scalable Bayesian Monte Carlo (SBMC), which bridges the gap between fast but heuristic methods and principled yet expensive samplers. It is a general method comprised of an approximate *model* and *algorithm* to simulate from the model. Our key insight is the model approximation π_s which features a scalar interpolation parameter $s \in [0, 1]$ that allows tuning between the MAP estimator ($s = 0$) and the full Bayesian posterior ($s = 1$). For smaller s the target is *easier to simulate from*, albeit with a larger bias with respect to the posterior. See the right panels of Figure 1. By simulating from this approximate target with *parallel* implementations of BMC algorithms, which we will denote by S-SMC $_{\parallel}$ and S-MCMC $_{\parallel}$, SBMC delivers strong performance in accuracy and UQ *at a comparable cost to SOTA methods like DE*. The prefix “S-” is for “scalable”, and the scalability comes from the model approximation *in tandem* with the parallelism, denoted by the subscript \parallel . Without the model approximation, the required simulation time is prohibitive.

Given data \mathcal{D} , the Bayesian posterior distribution over $\theta \in \Theta \subseteq \mathbb{R}^d$ is given by

$$\pi(\theta) \propto \mathcal{L}(\theta)\pi_0(\theta), \quad (1)$$

where $\mathcal{L}(\theta) := \mathcal{L}(\theta; \mathcal{D})$ is the likelihood of the data \mathcal{D} and $\pi_0(\theta)$ is the prior. The Bayes estimator of a quantity of interest $\varphi : \Theta \rightarrow \mathbb{R}$ is $\mathbb{E}[\varphi | \mathcal{D}] = \int_{\Theta} \varphi(\theta)\pi(\theta)d\theta$. It minimizes the appropriate Bayes risk at the population level and as such is Bayes optimal [MacKay, 1992, Neal, 2012, Andrieu et al., 2003, Bishop, 2006].

In general the posterior (target) distribution can only be evaluated up-to a constant of proportionality, and the available consistent methods for inference (learning) are of Monte Carlo type: notably Markov chain Monte Carlo (MCMC) [Metropolis et al., 1953, Hastings, 1970, Duane et al., 1987, Gelfand and Smith, 1990, Geyer, 1992, Robert et al., 1999, Roberts and Tweedie, 1996] and sequential Monte Carlo (SMC) samplers [Jarzynski, 1997, Berzuini and Gilks, 2001, Del Moral et al., 2006, Dai et al.,

³Autocorrelation function (ACF) and integrated autocorrelation time (IACT) are defined in Appendix E.2.

2022, Chopin et al., 2020]. The past several decades have seen enormous progress in methodology as well as practical applications [Galison et al., 2022, Mohan and Scaife, 2024], however standard implementations of these algorithms are still too expensive for practical BDL, and so BMC algorithms are typically used only as a benchmark for cheaper approximations [Izmailov et al., 2021]. See e.g. [Angelino et al., 2016, Papamarkou et al., 2024] for recent reviews and further references. The present work aims to address this computational intractability by (i) targeting an *approximation* of (1), and (ii) distributing the BMC workload across many workers in parallel. We will show that these two things together provide a *practical and scalable method*. The focus of the present work is on demonstrating the value of the SBMC method itself, independently of the particular BMC algorithm used, and so we mostly focus on standard implementations of HMC and SMC. But one of the virtues of SBMC is its extensibility: stochastic gradient MCMC methods Welling and Teh [2011], Chen et al. [2014] and/or other data-parallel techniques Angelino et al. [2016], Maclaurin and Adams [2014], Rendell et al. [2020] and more sophisticated adaptive methods Hoffman et al. [2021] can be swapped in later for additional gains.

The contributions of the present work are concisely summarized as follows:

- New SBMC method (e.g. S-SMC_{||} and S-MCMC_{||}) which allows the practitioner to *interpolate* between the MAP (or another point) estimator for $s = 0$ (0 additional simulation time) and the full posterior for $s = 1$ (long simulation time), thus balancing their UQ demands against their budget.
- A thorough systematic empirical evaluation of SBMC on several benchmarks demonstrates that it achieves excellent performance on both accuracy and UQ *at a cost comparable to DE, where traditional BMC methods fail severely*, demonstrating its strong scalability and robustness. See the top left panel of Figure 1.
- This benefit is illustrated on the downstream task of estimating prediction confidence, which can be used to improve safety and reliability. To that end, a meta-classifier is built using seven features of the SBMC posterior.

The paper is organized as follows. In Section 2, we introduce the SBMC method. In Section 3 we discuss its UQ abilities and the downstream task of output confidence prediction, as motivation, and present the main results. Section 4 discusses related literature. Section 5 presents the conclusion and additional discussion.

2 Scalable Bayesian Monte Carlo (SBMC) method

We define *time cost* as the required *simulation time per chain/particle*, and we will measure this by *epochs*, i.e. likelihood plus gradient evaluations, as a *hardware-agnostic proxy* for wall-clock time. Parallel implementations of consistent BMC algorithms like SMC_{||} and HMC_{||} improve time cost with near linear speed-up [Liang et al., 2025], but each process still needs to run for a long time, as seen in Figure 1 (c). This section introduces the model and algorithm choices that define the SBMC method in Algorithm 1, which delivers improved performance on metrics of interest for a *comparable time cost to deep ensembles*.

The model. Assume the prior is $\pi_0 = \mathcal{N}(0, V)$ for simplicity and define the MAP estimator as

$$\theta_{\text{MAP}} = \text{argmax}_{\theta} \mathcal{L}(\theta; \mathcal{D}) \pi_0(\theta),$$

where \mathcal{L} is the likelihood defined in equation (1). For a fixed tuning parameter $s \in (0, 1)$, we define $0 \prec \Sigma(s) = \Sigma(s)^T \in \mathbb{R}^{d \times d}$ and $\alpha(s) \in [0, 1]$, such that $\Sigma(0) = 0$ and $\Sigma(1) = V$, and $\alpha(0) = 1$ and $\alpha(1) = 0$. Define the new prior as

$$\bar{\pi}_0(\theta) = \mathcal{N}(\theta; \alpha(s)\theta_{\text{MAP}}, \Sigma(s)). \quad (2)$$

The SBMC method then targets the following distribution

$$\bar{\pi}(\theta) \propto \mathcal{L}(\theta)\bar{\pi}_0(\theta), \quad (3)$$

which we will refer to as the *anchored* posterior. We will refer to θ_{MAP} as the *anchor*.

For $s \rightarrow 0$, we recover a Dirac measure concentrated on the MAP estimator, which means no sampling is required. Conversely, as $s \rightarrow 1$, we recover the *original posterior*. Hence s is a scalar interpolation parameter which allows us to tune between these limits. For simplicity we will typically consider only the standard isotropic case $V = v\mathbf{I}$ and let $\alpha(s) = \mathbf{1}_{\{s < \frac{1}{2}\}}$ and $\Sigma = sv\mathbf{I}$.

We show that this approximate model balances the complementary strengths of the two approaches for small s , and enables BMC methods to deliver *scalable gains over alternatives like deep ensembles at a comparable cost*. The method is relatively insensitive to the exact value of s and we recommend a default value of $s = 0.1$. We will use the notation S-SMC $_{\parallel}$ and S-MCMC $_{\parallel}$ to distinguish the SBMC method from standard implementations of the algorithms targeting (1). For example, S-SMC $_{\parallel}$ means the SMC $_{\parallel}$ algorithm is used to sample from (3).

Algorithm 2 S-SMC sampler

Inputs: $\mathcal{L}, \bar{\pi}_0, N$.
 Init. $\theta_0^i \sim \bar{\pi}_0$ for $i = 1, \dots, N$. $Z^N = 1$.
for $j = 1$ **to** J (in serial) **do**
 (Optional) Select λ_j s.t. ESS = ρN , $\rho < 1$.
for $i = 1$ **to** N (in parallel) **do**
 Define $w_j^i \propto \tilde{w}_j^i \equiv \mathcal{L}(\theta_{j-1}^i)^{\lambda_j - \lambda_{j-1}}$.
Selection: $I_j^i \sim \{w_j^1, \dots, w_j^N\}$.
Mutation: $\theta_j^i \sim \mathcal{M}_j(\theta_{j-1}^{I_j^i}, \cdot)$.
end for
 Store $Z^N * = \frac{1}{N} \sum_{i=1}^N \tilde{w}_j^i$.
end for
Outputs: $\{\theta_J^i\}_{i=1}^N$ and Z^N .

The algorithm can be *any BMC method*. In the present work we will focus on SMC sampler and MCMC, but any alternative is admissible. For example, SG-MCMC or other methods which allow mini-batch gradients may be quite convenient for managing the memory requirements of very large problems.

SMC sampler. Define a sequence of intermediate targets $\bar{\pi}_j(\theta) \propto \mathcal{L}(\theta)^{\lambda_j} \bar{\pi}_0(\theta)$, according to a tempering schedule $0 = \lambda_0, \dots, \lambda_J = 1$, which will be chosen adaptively according to the effective sample size (ESS), as described in D.1 in the Appendix. The SMC sampler [Del Moral, 2004] alternates between *selection* by importance re-sampling, and *mutation* according to an appropriate intermediate MCMC transition kernel \mathcal{M}_j , such that $(\bar{\pi}_j \mathcal{M}_j)(d\theta) = \bar{\pi}_j(d\theta)$

[Geyer, 1992]. This operation must sufficiently de-correlate the samples, and as such we typically define the MCMC kernels \mathcal{M}_j by several steps of some basic MCMC kernel, leading to L_j epochs (likelihood/gradient evaluations). We will employ two standard MCMC kernels: preconditioned Crank-Nicolson (pCN) [Bernardo et al., 1998, Cotter et al., 2013] and Hamiltonian Monte Carlo (HMC) [Duane et al., 1987, Neal et al., 2011]. In the latter case, there are also several leapfrog steps for each HMC step contributing to L_j .

For a quantity of interest $\varphi : \Theta \rightarrow \mathbb{R}$, the S-SMC estimator from Algorithm 2 is given by

$$\bar{\pi}^N(\varphi) := \frac{1}{N} \sum_{i=1}^N \varphi(\theta^i) \xrightarrow{N \rightarrow \infty} \mathbb{E}_{\bar{\pi}}[\varphi] \approx \mathbb{E}_{\pi}[\varphi] = \mathbb{E}[\varphi \mid \mathcal{D}]. \quad (4)$$

S-SMC $_{\parallel}$ refers to P parallel executions of Algorithm 2, each with N particles, leading to a P times lower communication and memory overhead than a single S-SMC sampler with NP samples. This simplification is crucial for massive problems such as BDL, which require distributed architectures. Synchronous Single Instruction, Multiple Data (SIMD) resources can be used for the N communicating particles (and model- and data-parallel likelihood calculations), while all communication between the P processes is eliminated. The S-SMC $_{\parallel}$ ratio estimator is given as follows, for p i.i.d. realizations $\bar{\pi}^{N,p}(\varphi)$ of (4)

$$\hat{\varphi}_{\text{S-SMC}_{\parallel}} = \sum_{p=1}^P \omega_p \bar{\pi}^{N,p}(\varphi), \quad \omega_p = \frac{Z^{N,p}}{\sum_{p'=1}^P Z^{N,p'}}. \quad (5)$$

S-MCMC_{||} refers to P parallel executions of Algorithm 3, which already features N parallel short chains free from any communication. The purpose of formulating MCMC in this way is to match SMC, which itself features N parallel chains that need to communicate intermittently at the selection stage. The estimator is built exactly as (5), with $\{\theta^{i,p} = \theta_J^{i,p}\}_{i=1}^N$ in (4) and $Z^{N,p} = 1$.

3 Motivation and Results

UQ is a crucial pain-point for neural networks, and BDL is one of the leading contenders to deliver it. Our primary UQ metric will be *epistemic entropy*, which is the difference between *total* and aleatoric entropy, defined as follows [Hüllermeier and Waegeman, 2021, Depeweg et al., 2018, Shaker and Hüllermeier, 2020, Krause and Hübotter, 2025]

$$H_{\text{ep}}(x) = - \underbrace{\sum_{y \in \mathcal{Y}} \mathbb{E}[p(y|x, \theta)|\mathcal{D}] \log \mathbb{E}[p(y|x, \theta)|\mathcal{D}]}_{H_{\text{tot}}(x)} - \underbrace{\mathbb{E}\left[- \sum_{y \in \mathcal{Y}} p(y|x, \theta) \log(p(y|x, \theta))|\mathcal{D}\right]}_{H_{\text{al}}(x)}. \quad (6)$$

Aleatoric uncertainty is irreducible and can be thought of as label error (people may sometimes disagree on the label of a given hand-written digit), whereas epistemic entropy quantifies uncertainty which can be reduced with more data. Our focus is the latter, as it is *only* captured by Bayesian methods. It can be viewed as the mutual information between parameter and predictive posterior random variables for input x , and as such is 0 by definition for point estimators that yield deterministic predictive estimators.

Table 1: Comparison of methods on MNIST7 test data. SBMC methods are bold. For metrics, the best gold-standard (GS) value is bold, along with others within 1% for accuracy and NLL, and 50% for entropies (entropy is harder to estimate, and also high precision is less critical). SMC_{||}, HMC_{||}, and SGHMC_{||} are highlighted in red as they are particularly bad for these very short chains, and this is precisely the problem the approximate methods like SBMC address.

Method	P	Time Cost (epochs) ↓	Total Cost (epochs) ↓	Accuracy ↑	NLL ↓	H_{ep} correct	H_{ep} incorrect	H_{ep} OOD
MAP	1	160	160	92.3±0.366	0.253±0.012	0	0	0
SWA	1	160	160	92.3±0.387	0.27±0.017	0	0	0
MC Drop	1	160	160	93.9±0.626	0.214±0.021	0.049±0.007	0.269±0.008	0.267±0.01
Laplace	1	160	160	88.2±0.235	0.539±0.022	0.504±0.036	0.901±0.038	1.22±0.033
Deep Ens	1	176	1760	92.4±0.150	0.245±0.004	0.011±0.000	0.057±0.001	0.123±0.011
Deep Ens	8	178	14,240	92.5±0.059	0.239±0.001	0.011±0.000	0.059±0.001	0.134±0.004
SGHMC	1	160	1600	87.7±0.742	0.974±0.05	0.652±0.031	0.725±0.031	0.883±0.036
S-SGHMC	1	160 + 160	1760	90.3±0.758	0.409±0.014	0.342±0.015	0.687±0.027	0.836±0.039
S-SGHMC	8	160 + 160	12,960	92.3±0.160	0.388±0.001	0.434±0.005	0.782±0.007	0.965±0.003
SMC	1	173	1730	79.7±2.71	0.623±0.091	0.013±0.002	0.033±0.009	0.045±0.011
S-SMC	1	170 + 160	1860	92.2±0.371	0.267±0.014	0.026±0.003	0.129±0.014	0.202±0.028
S-SMC	8	178 + 160	14,400	93.3±0.160	0.226±0.004	0.059±0.001	0.272±0.003	0.378±0.03
HMC	1	160	1600	78.4±2.38	1.27±0.085	0.303±0.025	0.325±0.026	0.594±0.021
S-HMC	1	160 + 160	1760	93.0±0.166	0.232±0.002	0.056±0.001	0.264±0.002	0.463±0.009
S-HMC	8	160 + 160	12,960	93.1±0.085	0.231±0.002	0.070±0.000	0.299±0.002	0.531±0.011
HMC (GS)	1	20,000	20,000	93.6±0.415	0.222±0.009	0.096±0.004	0.410±0.013	0.768±0.084
HMC (GS)	1	200,000	200,000	94.8±0.211	0.194±0.004	0.120±0.004	0.493±0.008	1.04±0.122

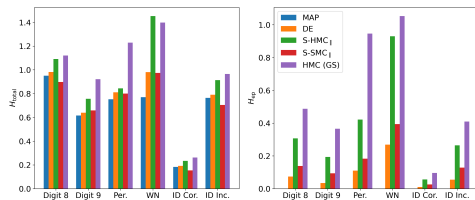


Figure 2: Average total and epistemic entropy over four OOD classes and correct and incorrect predictions ID for MNIST7 ($P = 1$). The average epistemic entropy over the test data, split by correct and incorrect predictions,

To illustrate the properties of SBMC, we conduct an experiment. The dataset is a subset of 1200 MNIST [LeCun et al., 2010] data trained on digits 0, ..., 7 (MNIST7) with 8, 9 held out as (similar but) out-of-domain (OOD). White noise inputs and randomly selected in-domain (ID) digits corrupted with white noise are considered as far OOD classes. The architecture is described in Appendix E.3.1. The prior variance is $v = 0.1$. The average total and epistemic entropy for various categories of OOD test data are presented in Figure 2 (per-digit result is given in Appendix F.1). The average epistemic entropy over the test data, split by correct and incorrect predictions,

are presented in Figure 2. This quantity is clearly predictive of misclassifications, and this downstream task will be revisited below.

In Table 1 we compare several SOTA competitors, including the **MAP** (computed with SGD and early stopping on validation data), **DE**, **MC Dropout**, **Laplace approximation**, and **SWA**, with **(S-)HMC \parallel** , **(S-)SMC \parallel** , and **(S-)SGHMC \parallel** all with *approximately equal time cost of ≈ 170 epochs*, according to SGD early stopping. These can be further parallelized with model- and data-parallel techniques, but we do not consider that here. Note that SBMC methods *require the MAP estimator*, so their total time cost is roughly **double**. A single HMC run using $2e4 - 2e5$ epochs is also included as a GS baseline. Convergence for all methods is verified by running 5 chains with dispersed initial conditions and measuring the standard error. Ensemble methods use P independent ensembles of $N = 10$ particles, and all particles are used for estimating posterior expectations.

The results show that when directly targeting (1), SMC_{\parallel} , HMC_{\parallel} , and SGHMC_{\parallel} , degrade rapidly away from convergence, to the point of **catastrophic failure** in first order metrics at this cost level. However, their UQ performance is still adequate—for example, some of the HMC_{\parallel} and SGHMC_{\parallel} H_{ep} estimators are within our tolerance of 50% of the GS solution (in bold). The MAP and DE quickly deliver good accuracy, but do not accurately estimate H_{ep} . These failure modes are perfectly *complementary*. To achieve the “best of both worlds”, SBMC anchors to the MAP estimator to preserve accuracy, and then uses an ensemble of short parallel runs of BMC to augment that with uncertainty. MC Dropout performs particularly well and is notably the only non-BMC method which achieves an H_{ep} estimator within our tolerance of 50% of the GS solution (in bold), and for a low total cost.

For the next experiments, we look at the IMDb sentiment classification dataset [Maas et al., 2011] and the CIFAR dataset [Krizhevsky et al., 2009]. Results for these cases are comparable and summarized in Figure 3 and Appendix F, along with further figures and tables. Further details on all model architectures are given in Appendix E.3. The next step is to apply the approach to LLMs—preliminary simulation results for next-token prediction with GPT-2 are given in Appendix A.1.

Table 2: Confidence meta-classifier results (optimal F_1 decision threshold, MNIST7).

P	Method	Precision	Recall	F_1	AUC-ROC
—	MAP	0.707	0.898	0.791	0.828
—	DE	0.734	0.897	0.807	0.855
1	S-SMC \parallel	0.701	0.890	0.783	0.824
8	S-SMC \parallel	0.753	0.915	0.826	0.884
1	S-HMC \parallel	0.750	0.906	0.820	0.885
8	S-HMC \parallel	0.752	0.913	0.825	0.892

to build a *confidence meta-classifier* of incorrect/OOD data, as follows. First, we fit our model to 1000 training data and 200 validation data for early stop procedure in MAP and DE methods/prior from MNIST7, and label incorrect predictions as $z = 1$ and correct predictions as $z = 0$. Then, we generate 2000 additional OOD meta-training data as described above, all of which get label $z = 1$. Let $p_{\text{max}}(x, \theta) := \max_y p(y|x, \theta) = p(y^*|x, \theta)$ denote the maximum probability, and denote the difference between the top two as $\Delta_{\text{max}}(x, \theta) := p_{\text{max}}(x, \theta) - \max_{y' \in \mathcal{Y} \setminus y^*} p(y|x, \theta)$. Let $p_{\text{max}}(x | \mathcal{D}) = \max_y \mathbb{E}[p(y|x, \theta) | \mathcal{D}]$. Consider as features:

$$p_{\text{max}}(x | \mathcal{D}), H_{\text{total}}(x), \mathbb{E}[p_{\text{max}}(x, \theta) | \mathcal{D}], \mathbb{E}[\Delta_{\text{max}}(x, \theta) | \mathcal{D}], H_{\text{ep}}(x), \text{Var}[p_{\text{max}}(x, \theta) | \mathcal{D}], \text{Var}[\Delta_{\text{max}}(x, \theta) | \mathcal{D}] .$$

Note that the last 3 are identically 0 for the MAP estimator, as they capture the epistemic uncertainty in the data. We build and standardize these features for each of our 4 models—MAP, DE, S-SMC \parallel ,



Figure 3: Accuracy, UQ, and confidence meta-classifier abstention (Abst) metrics (re-normalized so 1 is best) for IMDb (left) and CIFAR10 (right).

Out-of-domain inference. One clear application of UQ is inferring confidence in model predictions, i.e. whether the output is reliable or “hallucinated”, to borrow the vernacular from modern LLMs [Ji et al., 2023, Guo et al., 2025]. This information can be used to decide whether the model should abstain from responding or provided to the user so they can make their own decision about whether to trust the response. To that end, we propose

to build a *confidence meta-classifier* of incorrect/OOD data, as follows. First, we fit our model to 1000 training data and 200 validation data for early stop procedure in MAP and DE methods/prior from MNIST7, and label incorrect predictions as $z = 1$ and correct predictions as $z = 0$. Then, we generate 2000 additional OOD meta-training data as described above, all of which get label $z = 1$. Let $p_{\text{max}}(x, \theta) := \max_y p(y|x, \theta) = p(y^*|x, \theta)$ denote the maximum probability, and denote the difference between the top two as $\Delta_{\text{max}}(x, \theta) := p_{\text{max}}(x, \theta) - \max_{y' \in \mathcal{Y} \setminus y^*} p(y|x, \theta)$. Let $p_{\text{max}}(x | \mathcal{D}) = \max_y \mathbb{E}[p(y|x, \theta) | \mathcal{D}]$. Consider as features:

$S\text{-HMC}_{\parallel}$ and train the binary meta-classifier $x \mapsto z$, using a single hidden layer MLP with 50 neurons.

The results on 2000 ID test data plus 2000 newly-generated OOD test data are presented in Table 2. Accuracy is the ratio of true positives (not correct) and true negatives (correct) to the total testing dataset size. All estimators do surprisingly well, and our SBMC methods are the best. AUC-ROC is perhaps the most useful metric, as it measures the ability of the score $p_{\text{incorrect}}(x)$ to rank in-correctness of the subsequent inference: the probability that a randomly selected incorrect example from the test set, $x_{\text{incorrect}} \in \mathcal{D}_{\text{incorrect}}$ will have a higher score than a randomly selected correct example, $x_{\text{correct}} \in \mathcal{D}_{\text{correct}}$: $\mathbb{P}[p_{\text{incorrect}}(x_{\text{incorrect}}) > p_{\text{incorrect}}(x_{\text{correct}})]$.

Figure 4 shows the accuracy of a 2-level estimator over thresholds for IMDb. See Appendix G for further details. First we infer with the meta-classifier whether the model inference will be correct, under the assumption that OOD inputs implies incorrect inference. If yes, we infer with the original model. If no, we *abstain* from inference (abstentions are counted as correct decisions when the original model would be incorrect). Figure 3 presents summary metrics for IMDb and CIFAR10.

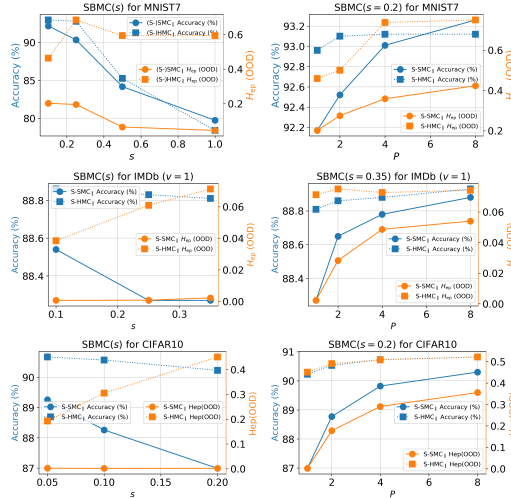


Figure 5: Dual axis Accuracy and $H_{ep}(\text{OOD})$ ablations over s in column 1 and P in column 2 for MNIST7 (row 1), IMDb (row 2), and CIFAR10 (row 3).

4 Discussion of Related Work

There has been a growing amount of work recently in many-short-chain MCMC, e.g. [Wilkinson, 2006, Chen et al., 2016, Sommer et al., 2024, Margossian et al., 2024, Nguyen et al., 2025, Sommer et al., 2025, Duffield et al., 2024]. The island-SMC method Vergé et al. [2015] considers interacting SMCs, which is necessary for consistency *unless the estimator is carefully constructed with appropriate weights* Whiteley et al. [2016], Dai et al. [2022]. See e.g. Liang et al. [2025] for further discussion.

The idea of *MAP-anchored priors* is intuitive, and closely related to a number of successful methods. In addition to augmenting data with adversarial perturbations of the inputs, as proposed in the original DE paper, another intuitive idea to promote spread and generalization is to randomize the model itself. Randomized maximum likelihood (RML) approaches do this by anchoring each ensemble member to random draws from the prior and/or data [Gu and Oliver, 2007, Bardsley et al., 2014, Pearce et al.,

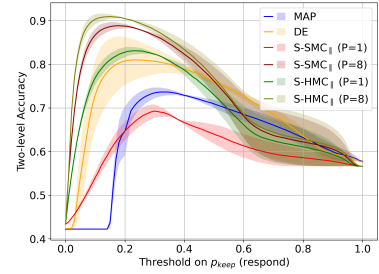


Figure 4: 2-level estimator (using confidence meta-classifier for abstention) accuracy on IMDb.

Ablations are considered by varying s and P . Small s improves mixing, as shown in Figure 1 (d), but also introduces bias because $\bar{\pi} \neq \pi$ (see (3), (1)). In this short-chain setting, smaller s typically increases accuracy and decreases $H_{ep}(\text{OOD})$. Both algorithms improve with P , but it is particularly notable that SMC_{||} improves much more. Comprehensive results are given in Appendix H.

Tuning. Firstly, we would like to emphasize that the results are fairly insensitive to $s \in [0.05, 0.3]$, and we recommend selecting $s = 0.1$ as a good default choice. It is worth noting that v is an important hyper-parameter *a priori*, at the level of the original Bayesian model. For example, changing from $v = 1/40$ to $v = 0.1$ for $s = 0.1$ changes (accuracy, NLL) from $(0.867, 0.365)$ to $(0.889, 0.271)$.⁴ If desired, one should first select v optimally for the MAP/DE, and then select s . Both can be done with CV. See Section 4 for further discussion.

⁴Prior tuning is relevant for *all methods*, and is not particular to SBMC.

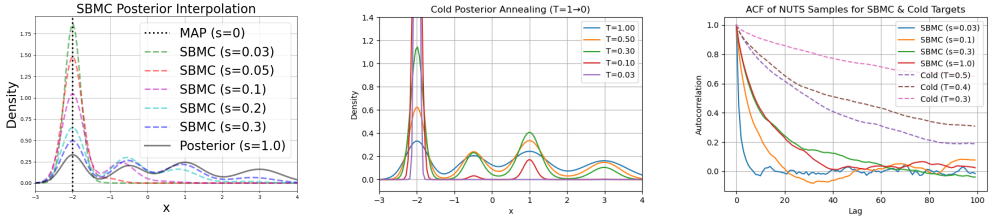


Figure 6: Left: SBMC for various s . Middle: Cold posterior for various T . Right: Autocorrelation functions using NUTS sampler, showing that SBMC *improves* mixing, while CP *hinders* mixing.

2020]. SBMC can easily bootstrap DE or RML ideas by initializing each process from a different MAP estimator. It is worth noting that MC Dropout Gal and Ghahramani [2016] could also do this.

The method most closely related to our work is Paulin et al. [2025], who anchor to the SWA estimator by adding a Gaussian factor, and simulate an ensemble of ULAs. They also observed an extreme speedup in mixing time. We experimented with a similar formulation with a factor of $\mathcal{N}(\theta_{\text{MAP}}, s\text{ld})$, $s \in (0, \infty)$, which also interpolates between the posterior and the MAP estimator and is arguably more elegant and theoretically appealing. But, the effective prior centers on $\frac{v}{s+v}\theta_{\text{MAP}}$ (or SWA), and in practice we found that this version did not perform as well as centering the prior on θ_{MAP} itself.

Cold posteriors [Wenzel et al., 2020] also interpolate between $\delta_{\theta_{\text{MAP}}}$ and the posterior via *annealing* (or ‘tempering’) the posterior (1) with an inverse temperature $T < 1$, as $\tilde{\pi}_T(\theta) \propto \mathcal{L}(\theta; \mathcal{D})^{1/T} \pi_0^{1/T}$. This *sharpens* the posterior, as shown in Figure 6 (middle) which typically makes the target distribution *more difficult to simulate and slows down* MCMC mixing, as shown in Figure 6 (right).

The SBMC likelihood is *effectively flattened relative to the Gaussian prior* by the factor s , while the missing information is represented in the sharper prior, as shown in Figure 6 (left). In practice, this means that the nonlinear and irregular component of the gradients has a smaller relative magnitude, the total Hessian of the posterior is better conditioned, and the chains mix faster. See Figure 6 (right) for an illustration of the mixing behavior, and Appendix C for further discussion, including a sketch of the mathematics. See Appendix B for discussion of other related works.

5 Conclusion

The SBMC method has been introduced and shown to be within reach of modern practical applications. It comprises a judicious **model** which uses a scalar parameter s to interpolate between $\delta_{\theta_{\text{MAP}}}$ ($s = 0$) and the posterior ($s = 1$), and is hence able to balance the benefits of each and achieve strong performance in accuracy and UQ metrics *at a cost comparable to SOTA approaches like DE*. Both MCMC $_{\parallel}$ and SMC $_{\parallel}$ are attractive **algorithm** options, which are consistent for the given target model. Therefore we have a mechanism for controlling the approximation between two reasonable choices if convergence is ensured. However, since the method no longer targets the posterior for any $s < 1$, we would recommend adopting a heuristic approach to convergence as with other SOTA methods, rather than chasing more rigorous convergence guarantees. Any BMC algorithm can be used, and SG-MCMC methods are particularly attractive since they are amenable to mini-batching and close to SGD, for which ample deep learning tooling is readily available. The next step is to apply the method to modern generative AI models [Guo et al., 2025, Agarwal et al., 2025, Bai et al., 2025, Huang et al., 2025] for controlling hallucinations and improving robustness and reliability. See Appendix A.1 for preliminary results on next-token prediction with GPT-2 and further discussion.

Acknowledgments and Disclosure of Funding

KJHL and XL gratefully acknowledge the support of IBM and EPSRC in the form of an Industrial Case Doctoral Studentship Award. JML acknowledges funding from the U.S. Department of Energy, Office of Science, Advanced Scientific Computing Research (Early Career Research Program, ReACT-QISE).

References

Sandhini Agarwal, Lama Ahmad, Jason Ai, Sam Altman, Andy Applebaum, Edwin Arbus, Rahul K Arora, Yu Bai, Bowen Baker, Haiming Bao, et al. gpt-oss-120b & gpt-oss-20b model card, 2025.

Christophe Andrieu, Nando De Freitas, Arnaud Doucet, and Michael I Jordan. An introduction to MCMC for machine learning. *Machine learning*, 50(1):5–43, 2003.

Elaine Angelino, Matthew James Johnson, Ryan P Adams, et al. Patterns of scalable Bayesian inference. *Foundations and Trends® in Machine Learning*, 9(2-3):119–247, 2016.

Gabriel Y Arteaga, Thomas B Schön, and Nicolas Pielawski. Hallucination detection in LLMs: Fast and memory-efficient finetuned models. *arXiv preprint arXiv:2409.02976*, 2024.

Shuai Bai, Keqin Chen, Xuejing Liu, Jialin Wang, Wenbin Ge, Sibo Song, Kai Dang, Peng Wang, Shijie Wang, Jun Tang, et al. Qwen2. 5-v1 technical report, 2025.

Rémi Bardenet, Arnaud Doucet, and Chris Holmes. On Markov chain Monte Carlo methods for tall data. *Journal of Machine Learning Research*, 18(47):1–43, 2017.

Johnathan M Bardsley, Antti Solonen, Heikki Haario, and Marko Laine. Randomize-then-optimize: A method for sampling from posterior distributions in nonlinear inverse problems. *SIAM Journal on Scientific Computing*, 36(4):A1895–A1910, 2014.

J Bernardo, J Berger, APAFMS Dawid, A Smith, et al. Regression and classification using Gaussian process priors. *Bayesian statistics*, 6:475, 1998.

Carlo Berzuini and Walter Gilks. Resample-move filtering with cross-model jumps. In *Sequential Monte Carlo methods in practice*, pages 117–138. Springer, 2001.

Christopher M Bishop. *Pattern recognition and machine learning*, volume 1. Springer, 2006.

Sid Black, Stella Biderman, Eric Hallahan, Quentin Anthony, Leo Gao, Laurence Golding, Horace He, Connor Leahy, Kyle McDonell, Jason Phang, et al. GPT-NeoX-20B: An open-source autoregressive language model. *arXiv preprint arXiv:2204.06745*, 2022.

Tianqi Chen, Emily Fox, and Carlos Guestrin. Stochastic gradient Hamiltonian Monte Carlo. In *International conference on machine learning*, pages 1683–1691. PMLR, 2014.

Yuxin Chen, David Keyes, Kody JH Law, and Hatem Ltaief. Accelerated dimension-independent adaptive Metropolis. *SIAM Journal on Scientific Computing*, 38(5):S539–S565, 2016.

Nicolas Chopin, Omiros Papaspiliopoulos, et al. *An introduction to sequential Monte Carlo*, volume 4. Springer, 2020.

Aakanksha Chowdhery, Sharan Narang, Jacob Devlin, Maarten Bosma, Gaurav Mishra, Adam Roberts, Paul Barham, Hyung Won Chung, Charles Sutton, Sebastian Gehrmann, et al. PaLM: Scaling language modeling with pathways. volume 24, pages 1–113, 2023.

Simon L Cotter, Gareth O Roberts, Andrew M Stuart, and David White. MCMC methods for functions: Modifying old algorithms to make them faster. *Statistical Science*, pages 424–446, 2013.

Chenguang Dai, Jeremy Heng, Pierre E Jacob, and Nick Whiteley. An invitation to sequential Monte Carlo samplers. *Journal of the American Statistical Association*, 117(539):1587–1600, 2022.

Erik Daxberger, Agustinus Kristiadi, Alexander Immer, Runa Eschenhagen, Matthias Bauer, and Philipp Hennig. Laplace redux-effortless Bayesian deep learning. volume 34, pages 20089–20103, 2021.

Pierre Del Moral. *Feynman-kac formulae*. Springer, 2004.

Pierre Del Moral, Arnaud Doucet, and Ajay Jasra. Sequential Monte Carlo samplers. *Journal of the Royal Statistical Society Series B: Statistical Methodology*, 68(3):411–436, 2006.

Stefan Depeweg, Jose-Miguel Hernandez-Lobato, Finale Doshi-Velez, and Steffen Udluft. Decomposition of uncertainty in Bayesian deep learning for efficient and risk-sensitive learning. In *International conference on machine learning*, pages 1184–1193. PMLR, 2018.

Simon Duane, Anthony D Kennedy, Brian J Pendleton, and Duncan Roweth. Hybrid Monte Carlo. *Physics letters B*, 195(2):216–222, 1987.

Samuel Duffield, Kaelan Donatella, Johnathan Chiu, Phoebe Klett, and Daniel Simpson. Scalable Bayesian Learning with posteriors. 2024.

Bradley Efron and Carl Morris. Stein’s estimation rule and its competitors—an empirical Bayes approach. *Journal of the American Statistical Association*, 68(341):117–130, 1973.

Runa Eschenhagen, Erik Daxberger, Philipp Hennig, and Agustinus Kristiadi. Mixtures of Laplace approximations for improved post-hoc uncertainty in deep learning. *arXiv preprint arXiv:2111.03577*, 2021.

Sebastian Farquhar, Jannik Kossen, Lorenz Kuhn, and Yarin Gal. Detecting hallucinations in large language models using semantic entropy. *Nature*, 630(8017):625–630, 2024.

Yarin Gal and Zoubin Ghahramani. Dropout as a Bayesian approximation: Representing model uncertainty in deep learning. In *international conference on machine learning*, pages 1050–1059. PMLR, 2016.

Peter Galison, Kazunori Akiyama, Antxon Alberdi, Walter Alef, Juan Carlos Algaba, Richard Anantua, Keiichi Asada, Rebecca Azulay, Uwe Bach, Anne-Kathrin Bacsko, et al. First Sagittarius A event horizon telescope results. iii. imaging of the galactic center supermassive black hole. *Astrophysical journal. Letters*, 930(2):L14, 2022.

Alan E Gelfand and Adrian FM Smith. Sampling-based approaches to calculating marginal densities. *Journal of the American statistical association*, 85(410):398–409, 1990.

Charles J Geyer. Practical Markov chain Monte Carlo. *Statistical science*, pages 473–483, 1992.

Walter R Gilks, Gareth O Roberts, and Edward I George. Adaptive direction sampling. *Journal of the Royal Statistical Society: Series D (The Statistician)*, 43(1):179–189, 1994.

Jonathan Goodman and Jonathan Weare. Ensemble samplers with affine invariance. *Communications in applied mathematics and computational science*, 5(1):65–80, 2010.

Priya Goyal, Piotr Dollár, Ross Girshick, Pieter Noordhuis, Lukasz Wesolowski, Aapo Kyrola, Andrew Tulloch, Yangqing Jia, and Kaiming He. Accurate, large minibatch SGD: Training ImageNet in 1 hour. *arXiv preprint arXiv:1706.02677*, 2017.

Yaqing Gu and Dean S Oliver. An iterative ensemble Kalman filter for multiphase fluid flow data assimilation. *Spe Journal*, 12(04):438–446, 2007.

David Gunawan, Khue-Dung Dang, Matias Quiroz, Robert Kohn, and Minh-Ngoc Tran. Subsampling sequential Monte Carlo for static Bayesian models. *Statistics and Computing*, 30(6):1741–1758, 2020.

Daya Guo, Dejian Yang, Haowei Zhang, Junxiao Song, Ruoyu Zhang, Runxin Xu, Qihao Zhu, Shirong Ma, Peiyi Wang, Xiao Bi, et al. Deepseek-r1: Incentivizing reasoning capability in llms via reinforcement learning. *arXiv preprint arXiv:2501.12948*, 2025.

Fredrik K Gustafsson, Martin Danelljan, and Thomas B Schon. Evaluating scalable Bayesian deep learning methods for robust computer vision. In *Proceedings of the IEEE/CVF conference on computer vision and pattern recognition workshops*, pages 318–319, 2020.

W Keith Hastings. Monte Carlo sampling methods using Markov chains and their applications. 1970.

Matthew Hoffman, Alexey Radul, and Pavel Sountsov. An adaptive-MCMC scheme for setting trajectory lengths in Hamiltonian Monte Carlo. In *International Conference on Artificial Intelligence and Statistics*, pages 3907–3915. PMLR, 2021.

Matthew D Hoffman and Pavel Sountsov. Tuning-free generalized Hamiltonian Monte Carlo. In *International conference on artificial intelligence and statistics*, pages 7799–7813. PMLR, 2022.

Matthew D Hoffman, Andrew Gelman, et al. The No-U-Turn sampler: adaptively setting path lengths in Hamiltonian Monte Carlo. *J. Mach. Learn. Res.*, 15(1):1593–1623, 2014.

Yupeng Hou, Jiacheng Li, Zhankui He, An Yan, Xiusi Chen, and Julian McAuley. Bridging language and items for retrieval and recommendation. *arXiv preprint arXiv:2403.03952*, 2024.

Edward J Hu, Yelong Shen, Phillip Wallis, Zeyuan Allen-Zhu, Yuanzhi Li, Shean Wang, Lu Wang, Weizhu Chen, et al. Lora: Low-rank adaptation of large language models. *ICLR*, 1(2):3, 2022.

Huang Huang, Fangchen Liu, Letian Fu, Tingfan Wu, Mustafa Mukadam, Jitendra Malik, Ken Goldberg, and Pieter Abbeel. Otter: A vision-language-action model with text-aware visual feature extraction. *arXiv preprint arXiv:2503.03734*, 2025.

Yanping Huang, Youlong Cheng, Ankur Bapna, Orhan Firat, Dehao Chen, Mia Chen, HyoukJoong Lee, Jiquan Ngiam, Quoc V Le, Yonghui Wu, et al. GPipe: Efficient training of giant neural networks using pipeline parallelism. volume 32, 2019.

Eyke Hüllermeier and Willem Waegeman. Aleatoric and epistemic uncertainty in machine learning: An introduction to concepts and methods. *Machine learning*, 110(3):457–506, 2021.

Pavel Izmailov, Dmitrii Podoprikhin, Timur Garipov, Dmitry Vetrov, and Andrew Gordon Wilson. Averaging weights leads to wider optima and better generalization. 2018.

Pavel Izmailov, Sharad Vikram, Matthew D Hoffman, and Andrew Gordon Gordon Wilson. What are Bayesian neural network posteriors really like? In *International conference on machine learning*, pages 4629–4640. PMLR, 2021.

Christopher Jarzynski. Equilibrium free-energy differences from nonequilibrium measurements: A master-equation approach. *Physical Review E*, 56(5):5018, 1997.

Ziwei Ji, Nayeon Lee, Rita Frieske, Tiezheng Yu, Dan Su, Yan Xu, Etsuko Ishii, Ye Jin Bang, Andrea Madotto, and Pascale Fung. Survey of hallucination in natural language generation. *ACM computing surveys*, 55(12):1–38, 2023.

Andreas Krause and Jonas Hübner. Probabilistic Artificial Intelligence. *arXiv preprint arXiv:2502.05244*, 2025.

Alex Krizhevsky, Geoffrey Hinton, et al. Learning multiple layers of features from tiny images. 2009.

Balaji Lakshminarayanan, Alexander Pritzel, and Charles Blundell. Simple and scalable predictive uncertainty estimation using deep ensembles. *Advances in neural information processing systems*, 30, 2017.

Yann LeCun, Corinna Cortes, and CJ Burges. Mnist handwritten digit database. *ATT Labs [Online]. Available: <http://yann.lecun.com/exdb/mnist>*, 2, 2010.

Xinzhu Liang, Joseph M Lukens, Sanjaya Lohani, Brian T Kirby, Thomas A Searles, Xin Qiu, and Kody JH Law. Comparison of parallel SMC and MCMC for Bayesian deep learning. *arXiv preprint arXiv:2402.06173*, 2025.

Andrew Maas, Raymond E Daly, Peter T Pham, Dan Huang, Andrew Y Ng, and Christopher Potts. Learning word vectors for sentiment analysis. In *Proceedings of the 49th annual meeting of the association for computational linguistics: Human language technologies*, pages 142–150, 2011.

David JC MacKay. A practical Bayesian framework for backpropagation networks. *Neural computation*, 4(3):448–472, 1992.

Dougal Maclaurin and Ryan P Adams. Firefly Monte Carlo: Exact MCMC with subsets of data. *arXiv preprint arXiv:1403.5693*, 2014.

Wesley J Maddox, Pavel Izmailov, Timur Garipov, Dmitry P Vetrov, and Andrew Gordon Wilson. A simple baseline for Bayesian uncertainty in deep learning. *Advances in neural information processing systems*, 32, 2019.

Charles C Margossian, Matthew D Hoffman, Pavel Sountsov, Lionel Riou-Durand, Aki Vehtari, and Andrew Gelman. Nested \hat{R} : assessing the convergence of Markov chain Monte Carlo when running many short chains. *Bayesian Analysis*, 1(1):1–28, 2024.

Nicholas Metropolis, Arianna W Rosenbluth, Marshall N Rosenbluth, Augusta H Teller, and Edward Teller. Equation of state calculations by fast computing machines. *The journal of chemical physics*, 21(6):1087–1092, 1953.

Devina Mohan and Anna MM Scaife. Evaluating Bayesian deep learning for radio galaxy classification. *arXiv preprint arXiv:2405.18351*, 2024.

Radford M Neal. *Bayesian learning for neural networks*, volume 118. Springer Science & Business Media, 2012.

Radford M Neal et al. MCMC using Hamiltonian dynamics. *Handbook of markov chain monte carlo*, 2(11):2, 2011.

Hanson H Nguyen, Kody JH Law, and Joseph M Lukens. Unorthodox parallelization for bayesian quantum state estimation. *New Journal of Physics*, 27(5):054507, 2025.

Theodore Papamarkou, Maria Skouliaridou, Konstantina Palla, Laurence Aitchison, Julyan Arbel, David Dunson, Maurizio Filippone, Vincent Fortuin, Philipp Hennig, José Miguel Hernández-Lobato, et al. Position: Bayesian deep learning is needed in the age of large-scale ai. In *International Conference on Machine Learning*, pages 39556–39586. PMLR, 2024.

Daniel Paulin, Peter A Whalley, Neil K Chada, and Benedict J Leimkuhler. Sampling from bayesian neural network posteriors with symmetric minibatch splitting langevin dynamics. In *International Conference on Artificial Intelligence and Statistics*, pages 5014–5022. PMLR, 2025.

Tim Pearce, Felix Leibfried, and Alexandra Brinstrup. Uncertainty in neural networks: Approximately Bayesian ensembling. In *International conference on artificial intelligence and statistics*, pages 234–244. PMLR, 2020.

Xin Qiu and Risto Miikkulainen. Semantic density: Uncertainty quantification for large language models through confidence measurement in semantic space. *Advances in neural information processing systems*, 37:134507–134533, 2024.

Xin Qiu, Elliot Meyerson, and Risto Miikkulainen. Quantifying point-prediction uncertainty in neural networks via residual estimation with an I/O kernel. *arXiv preprint arXiv:1906.00588*, 2019.

Samyam Rajbhandari, Jeff Rasley, Olatunji Ruwase, and Yuxiong He. ZeRO: Memory optimizations toward training trillion parameter models. In *SC20: International Conference for High Performance Computing, Networking, Storage and Analysis*, pages 1–16. IEEE, 2020.

Nils Reimers and Iryna Gurevych. Sentence-BERT: Sentence embeddings using siamese BERT-networks. *arXiv preprint arXiv:1908.10084*, 2019.

Lewis J Rendell, Adam M Johansen, Anthony Lee, and Nick Whiteley. Global consensus Monte Carlo. *Journal of Computational and Graphical Statistics*, 30(2):249–259, 2020.

Christian P Robert, George Casella, and George Casella. *Monte Carlo statistical methods*, volume 2. Springer, 1999.

Gareth O Roberts and Richard L Tweedie. Exponential convergence of Langevin distributions and their discrete approximations. 1996.

Mohammad Hossein Shaker and Eyke Hüllermeier. Aleatoric and epistemic uncertainty with random forests. In *International Symposium on Intelligent Data Analysis*, pages 444–456. Springer, 2020.

Mohammad Shoeybi, Mostafa Patwary, Raul Puri, Patrick LeGresley, Jared Casper, and Bryan Catanzaro. Megatron-LM: Training multi-billion parameter language models using model parallelism. 2019.

Emanuel Sommer, Lisa Wimmer, Theodore Papamarkou, Ludwig Bothmann, Bernd Bischl, and David Rügamer. Connecting the dots: Is mode-connectedness the key to feasible sample-based inference in bayesian neural networks? In *International Conference on Machine Learning*, pages 45988–46018. PMLR, 2024.

Emanuel Sommer, Jakob Robnik, Giorgi Nozadze, Uros Seljak, and David Rügamer. Microcanonical Langevin ensembles: advancing the sampling of Bayesian neural networks. 2025.

Kaitao Song, Xu Tan, Tao Qin, Jianfeng Lu, and Tie-Yan Liu. Mpnet: Masked and permuted pre-training for language understanding. *Advances in neural information processing systems*, 33: 16857–16867, 2020.

Saifuddin Syed, Alexandre Bouchard-Côté, Kevin Chern, and Arnaud Doucet. Optimised annealed Sequential Monte Carlo samplers. *arXiv preprint arXiv:2408.12057*, 2024.

Roman Vashurin, Ekaterina Fadeeva, Artem Vazhentsev, Lyudmila Rvanova, Daniil Vasilev, Akim Tsvigun, Sergey Petrakov, Rui Xing, Abdelrahman Sadallah, Kirill Grishchenkov, et al. Benchmarking uncertainty quantification methods for large language models with LM-polygraph. *Transactions of the Association for Computational Linguistics*, 13:220–248, 2025.

Christelle Vergé, Cyrille Dubarry, Pierre Del Moral, and Eric Moulines. On parallel implementation of sequential Monte Carlo methods: the island particle model. *Statistics and Computing*, 25(2): 243–260, 2015.

Jasper A Vrugt, Cajo JF Ter Braak, Cees GH Diks, Bruce A Robinson, James M Hyman, and Dave Higdon. Accelerating Markov chain Monte Carlo simulation by differential evolution with self-adaptive randomized subspace sampling. *International journal of nonlinear sciences and numerical simulation*, 10(3):273–290, 2009.

Max Welling and Yee W Teh. Bayesian learning via stochastic gradient Langevin dynamics. In *Proceedings of the 28th international conference on machine learning (ICML-11)*, pages 681–688, 2011.

Florian Wenzel, Kevin Roth, Bastiaan S Veeling, Jakub Świątkowski, Linh Tran, Stephan Mandt, Jasper Snoek, Tim Salimans, Rodolphe Jenatton, and Sebastian Nowozin. How good is the Bayes posterior in deep neural networks really? 2020.

Nick Whiteley, Anthony Lee, and Kari Heine. On the role of interaction in sequential Monte Carlo algorithms. 2016.

Darren J Wilkinson. Parallel Bayesian computation. *Statistics Textbooks and Monographs*, 184:477, 2006.

Andrew G Wilson and Pavel Izmailov. Bayesian deep learning and a probabilistic perspective of generalization. *Advances in neural information processing systems*, 33:4697–4708, 2020.

Kaichao You, Yong Liu, Jianmin Wang, and Mingsheng Long. LogME: Practical assessment of pre-trained models for transfer learning. In *International Conference on Machine Learning*, pages 12133–12143. PMLR, 2021.

Kaichao You, Yong Liu, Ziyang Zhang, Jianmin Wang, Michael I Jordan, and Mingsheng Long. Ranking and tuning pre-trained models: A new paradigm for exploiting model hubs. *Journal of Machine Learning Research*, 23(209):1–47, 2022.

A Future Directions

The most obvious next step is UQ for modern large language models (LLMs) [Guo et al., 2025], where robustness and hallucination detection are crucial pain points [Vashurin et al., 2025]. It has been recently shown that high-quality entropy metrics are valuable for identifying untrustworthy outputs there [Gustafsson et al., 2020, Arteaga et al., 2024, Farquhar et al., 2024]. In the context of LLMs, where the training itself is extremely computationally expensive, it becomes particularly important to have add-on plug-in type methods that can be applied post-training, such as [Qiu et al., 2019, Farquhar et al., 2024, Qiu and Miikkulainen, 2024]. But those methods are constrained to the uncertainty already encoded in the point estimator of model weights, which may already be under-estimated. The work [Arteaga et al., 2024] has shown that batch ensembles of fine-tuned LLMs can also work well for UQ hallucination detection, and also that epistemic uncertainty provides valuable information for that task. Based on existing benchmarks against deep ensembles, we believe our SBMC(s) approach will perform even better. Furthermore, an even simpler and cheaper version is to *learn the last layer* only, so all the data can be pre-processed once and for all by the frozen pre-trained LLM parameters, and then we simply run the last layer through SBMC. This can be applied at the pre-training or post-training stage, although the value of the method on downstream tasks will be most clear at post-training, while there would be some necessary design choices for how to leverage a pre-trained ensemble, instead of a point estimator, during post-training.

A.1 GPT-2

Here we present some preliminary results on GPT-2, on consumer hardware (an old MacBook Pro with an M2 processor and 16GB RAM). These are early results, just to further emphasize scalability and potential utility in hallucination detection. The starting point is the pre-trained GPT-2 model fine-tuned on Shakespeare data⁵. We then adopt a LoRA approach [Hu et al., 2022] to fine-tune an additive rank 50 adjustment with $\approx 2e5$ parameters at the last layer on the 3e5 token tiny Shakespeare dataset⁶ (in 128-token blocks) for 100 epochs, and consider top-1 token-level predictions⁷. The results are presented in Table 3.

Table 3: Comparison of methods on test accuracy, NLL, and various entropy metrics for next-token prediction with GPT2 on tiny Shakespeare.

Methods	Accuracy (%)	NLL	H_{tot} correct	H_{tot} incorrect	H_{ep} correct	H_{ep} incorrect
MAP	38.66	3.166	1.554	3.605	0	0
S-HMC	39.36	3.083	1.571	3.612	0.047	0.077

A.2 Overcoming other computational bottlenecks

Our sampler relies only on forward/back-prop evaluations, so every mainstream hardware scheme can be stacked on top of it: data-parallel all-reduce for moderate models[Goyal et al., 2017]; optimizer-state sharding (ZeRO/FSDP) when parameters no longer fit[Rajbhandari et al., 2020]; tensor model-parallelism for in-layer splits [Shoeybi et al., 2019] and pipeline model-parallelism for depthwise splits [Huang et al., 2019]; and, finally, the full hybrid of DP/sharding/tensor/pipeline that is now routine in trillion-parameter language models [Chowdhery et al., 2023, Black et al., 2022].

A.3 Further directions

Further directions at the methodological level include

- DE-SBMC: an obvious extension, would be to condition the HMC ensemble, or SMC ensemble ($P > 1$) with the DE, in case there may be any gain to be had.

⁵<https://huggingface.co/sadia72/gpt2-shakespeare>

⁶<https://raw.githubusercontent.com/karpathy/char-rnn/master/data/tinyshakespeare/input.txt>

⁷We truncated to the 2500 most frequent tokens, which includes tokens that appeared 11 or more times.

- One could condition SGLD/SGHMC with the MAP(s) from SGD (or DE). In this way, there is an initial phase which aims to recover a good point estimator, and then a second phase of essentially the same method, which aims to quantify the spread.
- P —parallelizing N —ensemble MCMC methods such as Gilks et al. [1994], Goodman and Weare [2010], Vrugt et al. [2009], Hoffman and Sountsov [2022].
- Leveraging N —ensemble MCMC methods within SMC for better mutations (with the cost of more communication).
- Parallel stochastic-gradient-MCMC methods like SGLD [Welling and Teh, 2011] and SGHMC [Chen et al., 2014], and ensembled versions thereof.
- Related to above, mini-batch gradients can be used in lieu of full gradients, which may have some advantages in terms of scalability and convergence. For SMC samplers, we have unbiased estimators $\widehat{\ell w}$ of log weights using mini-batches, and could use $\exp(\widehat{\ell w})$ for a non-negative and biased estimator or Bernoulli/Poisson augmentation to achieve (non-negative) unbiased weights [Gunawan et al., 2020, Bardenet et al., 2017].

B More related work

Empirical Bayes methods [Efron and Morris, 1973] fit higher level parameters in hierarchical models through optimization of the marginal likelihood. An SBMC model could be built in principle with a general prior $\pi_\phi(\theta)$, for example $\mathcal{N}(\theta; \mu, \Sigma)$ for $\phi = (\mu, \Sigma)$, and solved by EB. There is a significant cost overhead for optimizing the marginal-likelihood, but that could be offset in principle with Laplace approximation Bishop [2006] or other approaches. The particular SBMC(s) model considered here could also utilize EB for selecting s and/or α , as an alternative to cross-validation. And even before this, EB could be used to define the prior variance v , or a more general prior.

The work LogME You et al. [2021] use EB for fitting prior and likelihood variance in the context of transfer learning for regression, and then they extended this idea for building estimators from an ensemble of pre-trained models You et al. [2022]. The latter could naturally be combined with other ensemble approaches described above, and plugged into SBMC. The *Laplace Redux* work of Daxberger et al. [2021] provides an off-the-shelf Laplace module with block diagonal Hessian approximations to plug pre-trained models into for transfer learning. This could naturally augment SBMC in a number of ways, from leveraging it in marginal likelihood calculations for EB, to using it as a drop-in alternative for the prior, or leveraging their Hessian approximation in various other ways. It is worth momentarily digressing on an approach inspired by this observation. If the data is split into N_α pre-training and $N - N_\alpha$ fine-tuning sets, or if the likelihood is split by α and $1 - \alpha$ scalar fractions, then one could build a Laplace approximation (or another variational approximation) of the original α posterior, and use that as a prior for the remaining likelihood fraction. This posterior approximation may be closer to the original GS, and since each problem features an explicitly tempered likelihood, they should both be easier to solve. This may help with potentially overfitting, although we did not observe much of an issue in that respect.

C A sketch of the theory

We can think about the SBMC model as an incremental incorporation of the data. So first let $\sigma^2 = v/a$ and consider the original problem with prior $\mathcal{N}(0, \sigma^2)$. Now *split* the log-likelihood into $(1 - a)\ell + a\ell$, and consider incorporating *only the $a\ell$ part*. It is easy to see that the MAP estimator $\hat{\theta}_{\text{MAP}}$ for this problem is equivalent to the MAP estimator associated with the prior $\mathcal{N}(0, v)$. The *Laplace approximation* however, will differ, depending on which one we consider. Let us consider the $\mathcal{N}(0, \sigma^2)$ prior, and now it is time to incorporate the rest of the data $(1 - a)\ell$. The Hessian of our Laplace approximation is

$$a\nabla^2\ell(\theta) + \frac{1}{2(v/a)}\text{Id}.$$

This could be carried through rigorously, but for the sake of the argument, let's suppose we wave our hands and swap out $N_{\text{train}}\text{Id}$ for $\nabla^2\ell(\theta) = \sum_{i=1}^{N_{\text{train}}} \nabla^2\ell_i(\theta)$ (at least it is of the right order). To get back to the SBMC prior we have to equate

$$(2vN_{\text{train}} + 1)/(2v/a) = 1/(2sv) \quad \Rightarrow \quad a = s^{-1}/(2vN_{\text{train}} + 1).$$

Suppose $v = 0.1$ (common) and $s = 0.1$ (our recommendation). Then $a = 10/(N_{\text{train}}/5 + 1) \ll 1$, for large datasets. Therefore, $\ell \approx (1 - a)\ell$, and we end up with a reasonable approximation. Note this is also typically a positive thing for the prior, which is effectively $\mathcal{N}(0, \sigma^2 = v/a)$, since broader priors and less inductive bias typically deliver better performance, and small variance priors are often chosen more as a matter of convenience.

There are also immediate opportunities for extension, for example using better approximations of the Laplace approximation, or working out a more careful analysis along these lines.

Note that we can do things like this also to mitigate catastrophic forgetting in general when fine-tuning in a continual learning setting. Something similar was done for continual learning in Duffield et al. [2024]. Whereas, we do this simply to improve the approximation quality for short chains.

Hessian. Note the Hessian of the posterior π in (1) with $\mathcal{N}(0, v)$ prior is

$$\nabla^2 \ell + \frac{1}{v} \mathbf{Id}.$$

If we assume that the minimum eigenvalue of $\nabla^2 \ell$ is 0, and the maximum is λ_{\max} , then the *condition number* of the Hessian of the posterior is $\lambda_{\max} v + 1$. Meanwhile, the Hessian of the SBMC target $\bar{\pi}$ in (3) with $\mathcal{N}(\theta_{\text{MAP}}, vs)$ prior will have condition number $\lambda_{\max} vs + 1$. Therefore, the parameter $s < 1$ allows us to “tune away” the ill-conditioning of the posterior. See also the discussion in Paulin et al. [2025].

D Techniques for SMC_{||} in practice

Adaptive tempering. As mentioned, adaptive tempering is used to ensure a dense tempering regime and provide stability [Syed et al., 2024].

Example D.1 (Adaptive tempering). In order to keep the sufficient diversity of sample population, we let the effective sample size to be at least $\text{ESS}_{\min} = N/2$ at each tempering λ_{j-1} and use it compute the next tempering λ_j . For j th tempering, we have weight samples $\{w_{j-1}^k, \theta_{j-1}^k\}_{k=1}^N$, then the ESS is computed by

$$\text{ESS} = \frac{1}{\sum_{k=1}^N (w_{j-1}^k)^2},$$

where $w_{j-1}^k = \mathcal{L}(\theta_{j-1}^k)^{\lambda_j - \lambda_{j-1}} / \sum_{k=1}^N \mathcal{L}(\theta_{j-1}^k)^{\lambda_j - \lambda_{j-1}}$. Let $h = \lambda_j - \lambda_{j-1}$, the effective sample size can be presented as a function of h , $\text{ESS}(h)$. Using suitable root finding method, one can find h^* such that $\text{ESS}(h^*) = \text{ESS}_{\min}$, then set the next tempering $\lambda_j = \lambda_{j-1} + h^*$.

Note that the partition function estimator Z^N is no longer unbiased once we introduce adaptation, which means that in principle we should do short pilot runs and then keep everything fixed to preserve the integrity of the theory, but we have found this does not make a difference in practice.

Adaptive number of mutation steps. The number of mutation steps M is chosen adaptively. After resampling at a given tempering step, let $\theta^{i,0}$ denote the i -th sample and $\theta^{i,m}$ its state after m mutation steps. We monitor the mean displacement from the post-resampling state,

$$\text{dist}_m = \frac{1}{N} \sum_{i=1}^N \|\theta^{i,m} - \theta^{i,0}\|_2,$$

and terminate the mutation update at the smallest $M \geq 2$ for which the displacement has stabilized:

$$\frac{|\text{dist}_M - \text{dist}_{M-1}|}{\text{dist}_{M-1}} \leq \eta,$$

with tolerance $\eta > 0$. This criterion automatically increases M when the tempering increment is large or the target becomes tighter (requiring more mixing to decorrelate the resampled particles), and conversely saves computation when the resampled state is already close to stationary at the new tempering level.

Numerical stability: nested Log-sum-exp. When computing likelihoods in Sequential Monte Carlo (SMC) algorithms, numerical underflow frequently arises because likelihood values can become

extremely small, often beyond computational precision. To address this, one standard practice is to work with log-likelihoods rather than likelihoods directly. By operating in the log domain, the computer can safely store and manipulate extremely small values without loss of precision.

Specifically, the standard *log-sum-exp* trick can be applied to stabilize computations. For instance, consider a scenario with nested sums and products in parallel SMC. For each processor $p = 1, \dots, P$, we initially have:

$$Z^{N,p} = \prod_{j=1}^J \sum_{i=1}^N \omega_j^{i,p}.$$

To avoid numerical instability, each sum within the product is computed using the log-sum-exp trick:

$$\sum_{i=1}^N \omega_j^{i,p} = \exp \left(\max_i \log(w_j^{i,p}) \right) \sum_{i=1}^N \exp \left(\log(w_j^{i,p}) - \max_i \log(w_j^{i,p}) \right).$$

This procedure yields the decomposition:

$$Z^{N,p} = K^p \hat{Z}^p,$$

where

$$K^p = \prod_{j=1}^J \exp \left(\max_i \log(w_j^{i,p}) \right), \quad \text{and} \quad \hat{Z}^p = \prod_{j=1}^J \sum_{i=1}^N \exp \left(\log(w_j^{i,p}) - \max_i \log(w_j^{i,p}) \right).$$

In parallel SMC, an additional stabilization step is applied across processors. The global normalization constant across processors can also suffer from numerical instability. To address this, the log-sum-exp trick is applied again at the processor level:

$$Z^{N,p} = \exp \left(\log(\hat{Z}^p) + \log(K^p) - \log(K) \right) K,$$

with

$$\log(K) = \max_p \left(\log(\hat{Z}^p) + \log(K^p) \right).$$

Since the factor K cancels out when calculating the parallel SMC estimator, it suffices to compute only:

$$\exp \left(\log(\hat{Z}^p) + \log(K^p) - \log(K) \right),$$

which ensures numerical stability even when K itself is computationally very small.

Thus, by recursively applying the log-sum-exp trick at both the particle and processor levels, parallel SMC estimators can robustly handle computations involving extremely small numbers without numerical underflow.

E Complementary description of simulations

E.1 Computation of Error bars

Assume running R times of experiments to get R square errors/loss between simulated estimator $\hat{\varphi}$ and the ground truth, $\text{SE}(\hat{\varphi})^r$ for $r = 1, \dots, R$. Take the MSE as an example, the MSE is the mean of $\text{SE}(\hat{\varphi})^r$ over R realizations, and the standard error of MSE (s.e.) is computed by

$$\frac{\sqrt{\frac{1}{R} \sum_{r=1}^R (\text{SE}(\hat{\varphi})^r - \text{MSE})^2}}{\sqrt{R}}. \quad (7)$$

E.2 Integrated Autocorrelation Time

Integrated Autocorrelation Time (IACT) means the time until the chain is uncorrelated with its initial condition. The precise mathematical definition is as follows.

Let $\theta_0, \dots, \theta_t, \dots$ denote the Markov chain, and let $\varphi(\theta)$ be a scalar function of the state. We first define the *autocovariance function* (ACF) at lag s :

$$\gamma_s(\varphi) = \mathbb{E}[(\varphi(\theta_{t+s}) - \mathbb{E}[\varphi(\theta)])(\varphi(\theta_t) - \mathbb{E}[\varphi(\theta)])],$$

and the ACF at lag s as the normalized quantity

$$\rho_s(\varphi) = \frac{\gamma_s(\varphi)}{\gamma_0(\varphi)},$$

where $\gamma_0(\varphi)$ is the variance of $\varphi(\theta)$.

Then the *integrated autocorrelation time* (IACT) of φ is then defined in terms of the ACF by

$$\text{IACT}(\varphi) = 1 + 2 \sum_{s=1}^{\infty} \rho_s(\varphi).$$

E.3 Details of the Bayesian Neural Networks

Let weights be $A_i \in \mathbb{R}^{n_i \times n_{i-1}}$ and biases be $b_i \in \mathbb{R}^{n_i}$ for $i \in \{1, \dots, D\}$, we denote $\theta := ((A_1, b_1), \dots, (A_D, b_D))$. The layer is defined by

$$\begin{aligned} g_1(x, \theta) &:= A_1 x + b_1, \\ g_d(x, \theta) &:= A_d \sigma_{n_{d-1}}(g_{d-1}(x)) + b_d, \quad d \in \{2, \dots, D-1\}, \\ g(x, \theta) &:= A_D \sigma_{n_{D-1}}(g_{D-1}(x)) + b_D, \end{aligned}$$

where $\sigma_i(u) := (\nu(u_1), \dots, \nu(u_i))^T$ with ReLU activation $\nu(u) = \max\{0, u\}$.

Consider the discrete data set in a classification problem, we have $\mathbb{Y} = \{1, \dots, K\}$ and $n_D = K$, then we instead define the so-called *softmax* function as

$$h_k(x, \theta) = \frac{\exp(g_k(x, \theta))}{\sum_{j=1}^K \exp(g_j(x, \theta))}, \quad k \in \mathbb{Y}, \quad (8)$$

and define $h(x, \theta) = (h_1(x, \theta), \dots, h_K(x, \theta))$ as a categorical distribution on K outcomes based on data x . Then we assume that $y_i \sim h(x_i)$ for $i = \{1, \dots, m\}$.

Now we describe the various neural network architectures we use for the various datasets.

E.3.1 MNIST7 Classification Example

The architecture is a simple CNN with (i) one hidden layer with 4 channels of 3×3 kernels with unit stride and padding, followed by (ii) ReLU activation and (iii) 2×2 max pooling, (iv) a linear layer, and (v) a softmax. The parameter prior and dataset is built as follows

- Training is conducted on a sub-dataset consisting of the first 1200 training samples with labels 0 through 7. Evaluation is performed on first N_{id} in-domain test images with labels 0 through 7 and the on the four generated out-of-domain dataset (N_{ood} total number of data).
- The OOD dataset is generated as follows: two of the datasets are the first $N_{\text{ood}}/4$ out-of-domain test images with labels 8 and 9, respectively. The third dataset, the white noise image (wn), is a set of $N_{\text{ood}}/4$ synthetic 28×28 “images” with pixels drawn uniformly at random from $[0, 1]$. The fourth dataset, the perturbed image (per.), is a set of the first $N_{\text{ood}}/4$ MNIST test images of digits 0–7, each pixel perturbed by Gaussian noise (standard error as 0.5) while retaining its original label.
- MAP and DE are estimated using an initialization and regularization based on the prior $N(0, v/d)$, where $d = 6320$ and $v = 0.1$. The tuning parameter in SBMC methods is s . The batchsize is 64.

- The gold-standard is computed by the single HMC over 5 realizations, called HMC (GS), with $N = B, T = 1$ and $L = 1$.
- SWA. Starting from the estimated MAP weights, we train with SGD (momentum 0.9, lr 10^{-3}). After a 25-epoch warm-up, we update an `AveragedModel` each epoch (1 weight sample per epoch) and use `SWALR` with $\text{swa_lr} = 5 \times 10^{-4}$. After training we use the SWA weights for prediction. We run $R=5$ independent replicates.
- MC Dropout. We enable a 30% dropout in the (only) dropout layer after flattening (before the FC). Starting from the MAP estimation, we train with Adam (lr 10^{-3}). At test time, we keep dropout on and average $T=10$ stochastic forward passes for predictive probabilities. We run $R=5$ independent replicates.
- Laplace. We fit a Laplace approximation with a Kronecker-factored approximation of the Hessian⁸Daxberger et al. [2021]. The starting model is the estimated MAP model; we estimate the posterior over the last layer and draw $T=10$ predictive weight samples with `pred_type='nn'` (re-linearization) for MC predictive inference. We run $R=5$ independent replicates.

E.3.2 IMDb Classification Example

Here we use SBERT embeddings Reimers and Gurevych [2019] based on the model `all-mpnet-base-v2` Song et al. [2020]⁹. In other words, frozen weights from `all-mpnet-base-v2` until the 768 dimensional [CLS] output. The NN model and parameter prior for IMDb¹⁰ are built as follows

- NN is followed by (i) no hidden layer, (ii) ReLU activation, (iii) a final linear layer, and (iv) softmax output.
- Training is conducted on the whole train set (25000 data). Evaluation is performed on the whole test images as the in-domain dataset (25000 data) and on the four generated out-of-domain datasets (N_{ood} total number of data).
- The OOD dataset is generated as follows: four of these datasets (each dataset has $N_{\text{ood}}/5$ data) use textual data from the Appliances domain, which is distinct from the in-domain IMDb movie review data. Specifically, four OOD datasets were constructed from Amazon Reviews 2023 Appliances data Hou et al. [2024]¹¹, containing customer reviews and product metadata. Two datasets directly used the two JSON files, and two text-based OOD datasets were generated as follows. From `Appliances.jsonl`, we extracted the review text, representing natural language expressions of user opinions but unrelated to movies; from `meta_Appliances.jsonl`, we constructed meta descriptions by concatenating each product's title and listed features. The last dataset, Lipsum, is a collection of 100 very short, meaningless text strings, each consisting of between one and ten randomly selected words drawn from the classic “Lorem ipsum” filler vocabulary.
- MAP and DE are estimated using an initialization and regularization based on the prior $N(0, v\text{ld})$, where $d = 1538$. The tuning parameter in SBMC methods is s . The batchsize is 64.
- The gold-standard is computed by the single HMC over 5 realizations, called HMC (GS), with $N = B, T = 1$ and $L = 1$.

E.3.3 CIFAR-10 Classification Example

Here, the architecture is ResNet-50 pre-trained from ImageNet with all parameters frozen until the final pooled 2048 dimensional features. The NN model and parameter prior for CIFAR10 are as follows.

- NN is followed by (i) no hidden layer, (ii) ReLU activations, (iii) a final linear layer, and (iv) softmax output.

⁸<https://github.com/aleximmer/Laplace>

⁹<https://huggingface.co/sentence-transformers/all-mpnet-base-v2>

¹⁰<https://huggingface.co/datasets/stanfordnlp/imdb>

¹¹<https://amazon-reviews-2023.github.io/>

- Training is conducted on the whole train set (50000 data). Evaluation is performed on the whole test images as the in-domain dataset (10000 data) and on the three generated out-of-domain datasets (N_{ood} total number of data).
- The OOD dataset is generated as follows:
 - Close OOD (CIFAR-100 “not in CIFAR-10”). Drawn $N_{\text{ood}}/3$ data from the 90 fine-grained CIFAR-100 classes that don’t overlap with the 10 classes inCIFAR-10. All images are 32×32 RGB natural photographs with nearly identical color distribution and textures to CIFAR-10.
 - Corrupt OOD (CIFAR-10-C). Select $N_{\text{ood}}/3$ CIFAR-10 test images and subject them to 15 types of realistic distortions—Gaussian/impulse noise (motion/defocus blur, frost, fog, brightness/contrast shifts, JPEG compression, pixelation, etc.) at five different severity levels. The pixel-level statistics are methodically disturbed, yet the original labels stay the same.
 - Far OOD (SVHN). Select $N_{\text{ood}}/3$ data from 26032 32x32 RGB test photos of house-number digits (0–9) that have been cut from Google Street View. The SVHN displays centred white numbers on colourful, frequently cluttered urban backgrounds, in contrast to CIFAR’s multi-object array of natural-scene photos.
- MAP and DE are estimated using an initialization and regularization based on the prior $N(0, v\mathbf{I}_d)$, where $d = 20490$ and $v = 0.2$. The tuning parameter in SBMC methods is s . The batchsize is 128.
- The gold-standard is computed by the single HMC over 5 realizations, called HMC (GS), with $N = B, T = 1$ and $L = 1$.

E.4 Hardware description

The main CPU cluster we access has nodes with 2×16 -core Intel Skylake Gold 6130 CPU @ 2.10GHz, 192GB RAM *without communication* in between, so it can only run $N/P = 32$ particles in parallel with one particle per core. There are also unconnected AMD “Genoa” compute nodes, with 2×84 -core AMD EPYC 9634 CPUs and 1.5TB RAM.

F Further results for UQ

Results in this section further support the statement mentioned in the main text, that is, (i) SBMC significantly outperforms the MAP estimator, as well as a DE of MAP estimators, (ii) DE systematically underestimates H_{ep} for the same ensemble size as SBMC.

F.1 MNIST7

In the MNIST7 case, the full setting is described in Appendix E.3.1, where we let $N_{\text{id}} = 7000$ and $N_{\text{ood}} = 2000$, where each dataset has 500 data. Selected results appear in the main text in Figure 2, where the full data table is given in Table 16. Additional detailed results of the per-digit analysis are provided below, see Figure 7, and the full data table in Table 12.

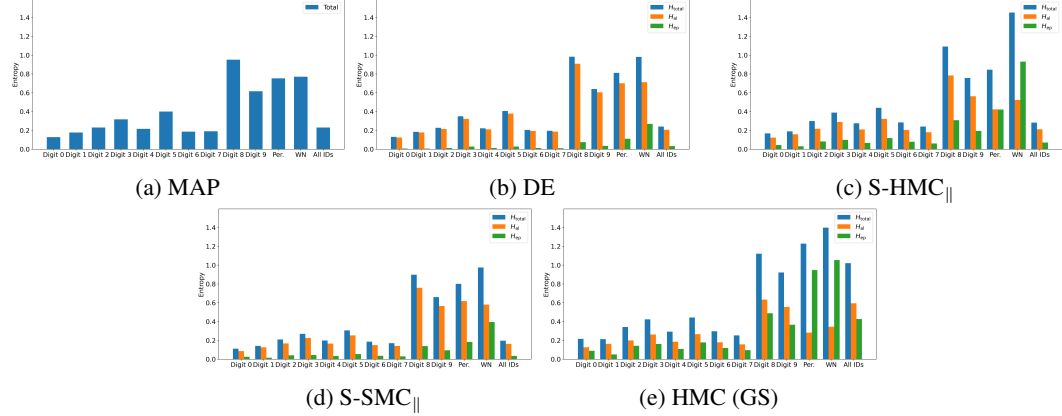


Figure 7: Comparison of entropy across groups for MNIST7. S-SMC_{||} ($P = 1$ chain with $N = 10$), S-HMC_{||} (NP chains), HMC (GS) ($2e4$ samples), DE (N models) and MAP, with fixed number of leapfrog $L = 1$, $v = 0.1$ and $s = 0.1$ (5 realizations).

F.2 IMDb

In the IMDb case, the full setting is described in Appendix E.3.2, where we let $N_{\text{ood}} = 500$, and each dataset has 100 data.

Experiments with $v = \frac{1}{40}$. Results of entropy comparison among MAP, DE and SBMCs are given in Figure 8, showing comparison in the OOD datasets and the correct/incorrect predictions in the ID domain. Additional detailed results of the per-digit analysis are provided below, see Figure 9, and the full data table in Table 13.

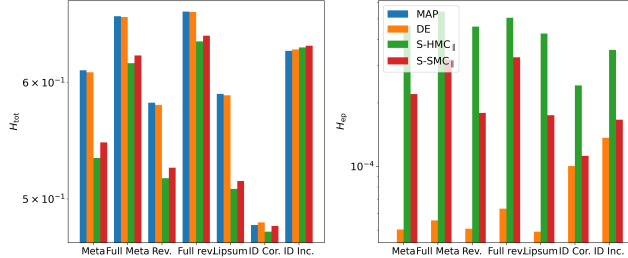


Figure 8: Comparison of average total and epistemic entropy over four out-of-domain classes and correct/incorrect predictions in-domain for IMDb. S-SMC_{||} ($P = 1$ chain with $N = 10$), S-HMC_{||} (NP chains), DE (N models) and MAP, with fixed number of leapfrog $L = 1$, $B = 25$, $M = 1$, $v = 0.025$ and $s = 0.1$ (5 realizations).

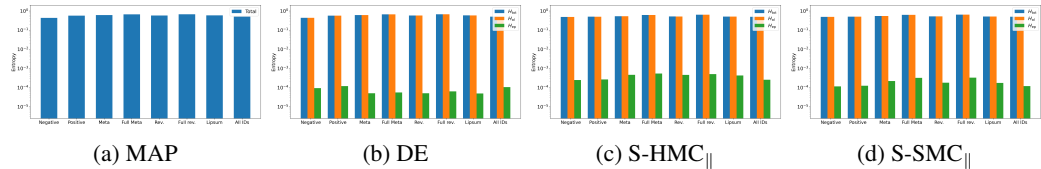


Figure 9: Comparison of entropy across groups for IMDb. S-SMC_{||} ($P = 1$ chain with $N = 10$), S-HMC_{||} (NP chains), DE (N models) and MAP, with fixed number of leapfrog $L = 1$, $B = 25$, $M = 1$, $v = 0.025$ and $s = 0.1$ (5 realizations).

Experiments with $v = 1$. Results of entropy comparison among MAP, DE and SBMCs are given in Figure 10, showing comparison in the OOD datasets and the correct/incorrect predictions in the ID

domain. Additional detailed results of the per-digit analysis are provided below, see Figure 11, and the full data table in Table 14.

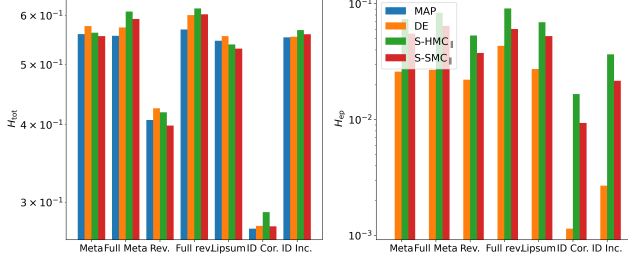


Figure 10: Comparison of average total and epistemic entropy over four out-of-domain classes and correct/incorrect predictions in-domain for IMDb. S-SMC_{||} ($P = 8$ chain with $N = 10$), S-HMC_{||} (NP chains), DE (N models) and MAP, with fixed number of leapfrog $L = 1$, $B = 26$, $M = 2$, $v = 1$ and $s = 0.35$ (5 realizations).

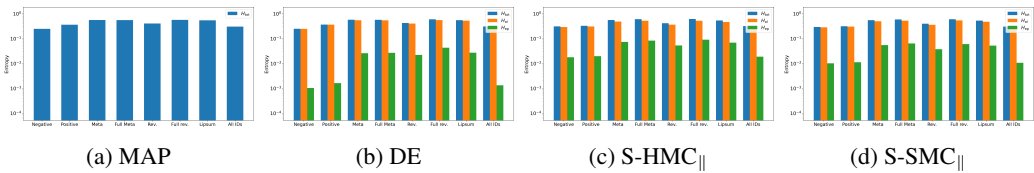


Figure 11: Comparison of entropy across groups for IMDb. S-SMC_{||} ($P = 8$ chain with $N = 10$), S-HMC_{||} (NP chains), DE (N models) and MAP, with fixed number of leapfrog $L = 1$, $B = 26$, $M = 2$, $v = 1$ and $s = 0.35$ (5 realizations).

F.3 CIFAR10

In the CIFAR10 case, the full setting is described in Appendix E.3.3, where we let $N_{\text{id}} = 10000$ and $N_{\text{ood}} = 300$, and each dataset has 100 data points. Results of entropy comparison among MAP, DE and SBMCs are given in Figure 12, showing comparison in the OOD datasets and the correct/incorrect prediction in the ID domain.

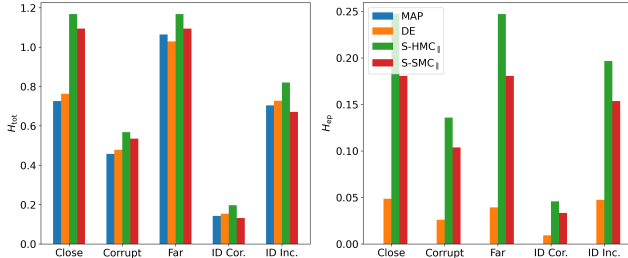


Figure 12: Comparison of average total and epistemic entropy over three out-of-domain classes and correctly/incorrectly predicted ID for CIFAR10. S-SMC_{||} ($P = 8$ chains with $N = 10$), S-HMC_{||} (NP chains), DE (N) and MAP, with fixed number of leapfrog $L = 1$, $B = 200$, $M = 4$, $v = 0.2$ and $s = 0.05$ (5 realizations).

G Further results of OOD inference

Establishment of the meta-classifier of incorrect/OOD data is given in the main text under Out-of-domain inference. Here, the OOD detection is performed in the default and optimal F_1 decision rule, respectively.

The default decision rule treats the output probability of "abstain" (out-of-domain or likely misclassified) in the meta-classifier as a binary decision with a fixed cut-off at 0.5. That is, if the model predicts that there is at least a 50% probability of the data being OOD or incorrectly predicted, it abstains; otherwise, it classifies the data as correctly predicted ID. This rule requires no adjustment beyond the choice of 0.5. Its behaviour is totally dependent on whether the model's confidence in abstention exceeds the halfway level.

The optimal F_1 decision rule adapts the abstention threshold to maximize the F_1 score on a held-out set. In practice, the meta-classifier's probabilities are assessed over a grid of potential thresholds ranging from 0 to 1, the F_1 score are calculated for each threshold, and the threshold with the highest F_1 score is chosen as the optimal F_1 threshold. This customised threshold balances false positives and false negatives in the most effective way for the given data distribution, at the cost of requiring a representative validation set. It often outperforms the default decision rule when class proportions or costs of errors are skewed.

G.1 MNIST7

In the MNIST7 case, the full setting is described in Appendix E.3.1, where we let $N_{\text{id}} = 2000$ and $N_{\text{ood}} = 2000$, where each dataset has 500 data. Metrics of Precision, Recall, F_1 and AUC-ROC metrics are given in Table 4, the normalized confusion rate matrices to show how the OOD domain has been detected from the ID domain are given in Figure 13. Plots for ROC curve and 2-level estimator accuracy are given in Figure 14.

Table 4: Evaluation Metrics using thresholds. S-SMC $_{\parallel}$ ($P = 1, 8$ chains with $N = 10$) and S-HMC $_{\parallel}$ (NP chains), with fixed number of leapfrog $L = 1, B = 160, M = 10, v = 0.1$ and $s = 0.1$, on MNIST (5 realizations, \pm s.e. in metrics and bold the first 30% data in mean).

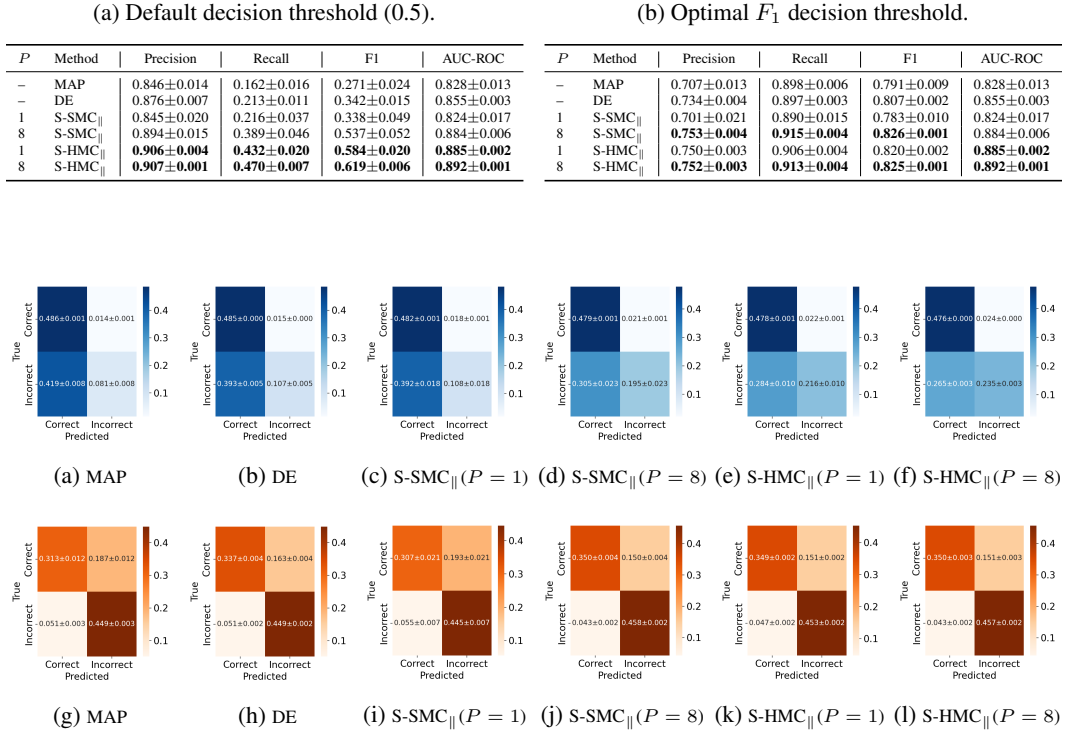


Figure 13: Averaged confusion rate matrices for OOD prediction on MNIST7, with default decision threshold (top) and optimal F_1 decision threshold (bottom). S-SMC $_{\parallel}$ ($P = 1, 8$ chains with $N = 10$) and S-HMC $_{\parallel}$ (NP chains), with fixed number of leapfrog $L = 1, B = 160, M = 10, v = 0.1$ and $s = 0.1$, on MNIST (5 realizations and \pm s.e. in metrics).

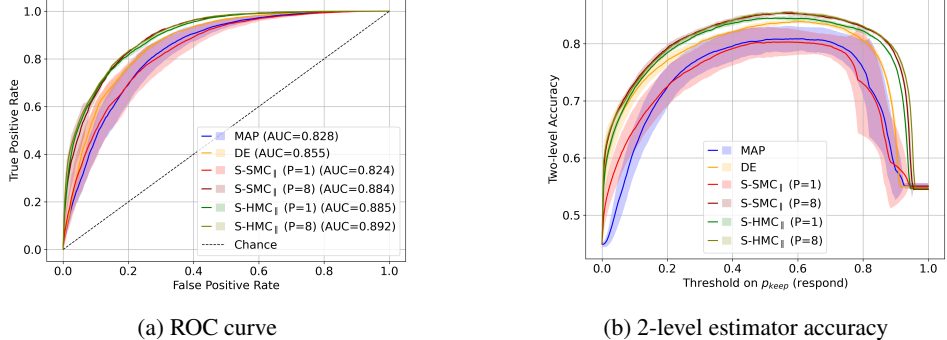


Figure 14: Averaged curve plots for OOD detection on MNIST7. S-SMC_{||} ($P = 1, 8$ chains with $N = 10$) and S-HMC_{||} (NP chains), with fixed number of leapfrog $L = 1$, $B = 160$, $M = 10$, $v = 0.1$ and $s = 0.1$, on MNIST (5 realizations and \pm s.e. in metrics).

G.2 IMDB

In the IMDb case, the full setting is described in Appendix E.3.2, where we let $N_{\text{ood}} = 25000$, and each dataset has 5000 data points.

Experiment with $v = \frac{1}{40}$ Metrics of Precision, Recall, F1 and AUC-ROC metrics are given in Table 5, the normalized confusion rate matrices to show how the OOD domain has been detected from ID domain are given in Figure 15. Plots for ROC curve and 2-level estimator accuracy are given in Figure 16.

Table 5: Performance at the optimal F_1 decision threshold. S-SMC_{||} ($P = 1$ chain with $N = 10$), S-HMC_{||} (NP chains), DE (N models) and MAP, with fixed number of leapfrog $L = 1$, B , M , $v = 0.025$ and $s = 0.1$ (5 realizations, \pm s.e. in metrics and bold the first 30% data in mean).

P	Method	Precision	Recall	F1	AUC-ROC
–	MAP	0.707 ± 0.003	0.953 ± 0.001	0.811 ± 0.001	0.768 ± 0.005
–	DE	0.856 ± 0.041	0.890 ± 0.017	0.869 ± 0.016	0.896 ± 0.025
1	S-SMC	0.673 ± 0.005	0.919 ± 0.002	0.777 ± 0.004	0.777 ± 0.002
8	S-SMC	0.935 ± 0.003	0.876 ± 0.002	0.905 ± 0.000	0.935 ± 0.002
1	S-HMC	0.844 ± 0.002	0.876 ± 0.004	0.859 ± 0.001	0.905 ± 0.001
8	S-HMC	0.970 ± 0.003	0.879 ± 0.003	0.922 ± 0.000	0.944 ± 0.002

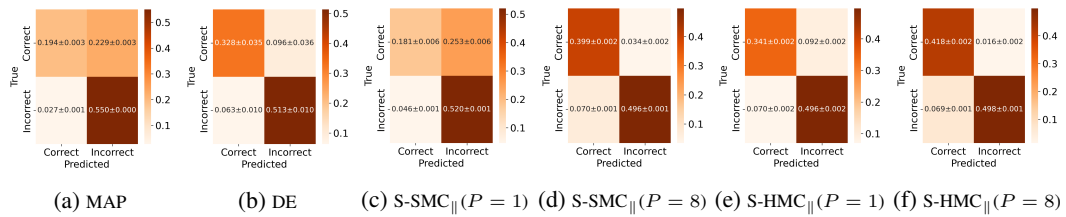


Figure 15: Averaged confusion rate matrices for OOD prediction on IMDb, with optimal F_1 decision threshold. S-SMC_{||} ($P = 1, 8$ chain with $N = 10$), S-HMC_{||} (NP chains), DE (N models) and MAP, with fixed number of leapfrog $L = 1$, $B = 25$, $M = 1$, $v = 0.025$ and $s = 0.1$ (5 realizations and \pm s.e. in metrics).

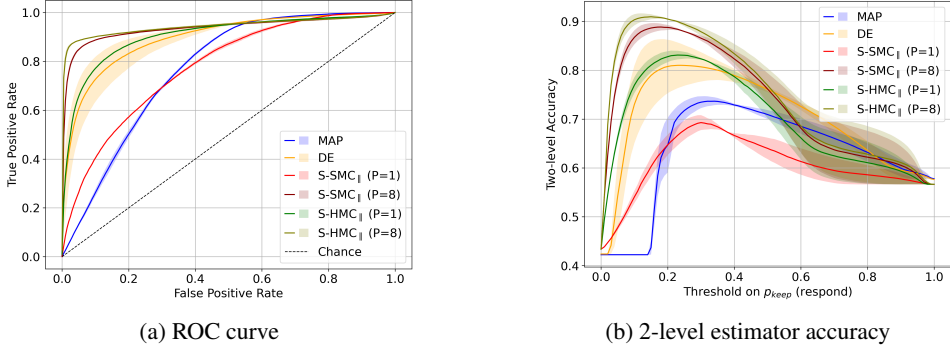


Figure 16: Averaged curve plots for OOD detection in IMDb. S-SMC_{||} ($P = 1, 8$ chain with $N = 10$), S-HMC_{||} (NP chains), DE (N models) and MAP, with fixed number of leapfrog $L = 1$, $B = 25$, $M = 1$, $v = 0.025$ and $s = 0.1$ (5 realizations and \pm s.e. in metrics).

Experiment with $v = 1$. Metrics of Precision, Recall, F1 and AUC-ROC metrics are given in Table 6, the normalized confusion rate matrices to show how the OOD domain has been detected from the ID domain are given in Figure 17. The plots for the ROC curve and 2-level estimator accuracy are given in Figure 18.

Table 6: Performance at the optimal F_1 decision threshold. S-SMC_{||} ($P = 1$ chain with $N = 10$), S-HMC_{||} (NP chains), DE (N models) and MAP, with fixed number of leapfrog $L = 1$, B , M , $v = 1$ and $s = 0.35$ (5 realizations, \pm s.e. in metrics and bold the first 30% data in mean).

P	Method	Precision	Recall	F1	AUC-ROC
—	MAP	0.733 ± 0.004	0.897 ± 0.003	0.807 ± 0.002	0.809 ± 0.006
—	DE	0.968 ± 0.004	0.880 ± 0.004	0.922 ± 0.001	0.959 ± 0.003
1	S-SMC	0.791 ± 0.000	0.871 ± 0.003	0.829 ± 0.001	0.889 ± 0.001
8	S-SMC	0.947 ± 0.003	0.878 ± 0.003	0.911 ± 0.000	0.944 ± 0.002
1	S-HMC	0.923 ± 0.002	0.885 ± 0.001	0.904 ± 0.001	0.943 ± 0.002
8	S-HMC	0.965 ± 0.004	0.880 ± 0.003	0.920 ± 0.000	0.948 ± 0.002

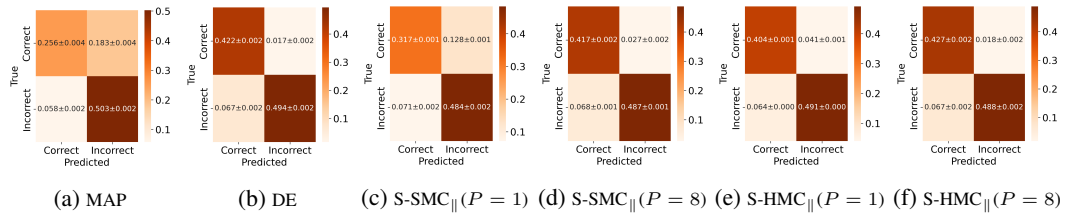


Figure 17: Averaged confusion rate matrices for OOD prediction on IMDb, with optimal F_1 decision threshold. S-SMC_{||} ($P = 1, 8$ chain with $N = 10$), S-HMC_{||} (NP chains), DE (N models) and MAP, with fixed number of leapfrog $L = 1$, $B = 26$, $M = 2$, $v = 1$ and $s = 0.35$ (5 realizations and \pm s.e. in metrics).

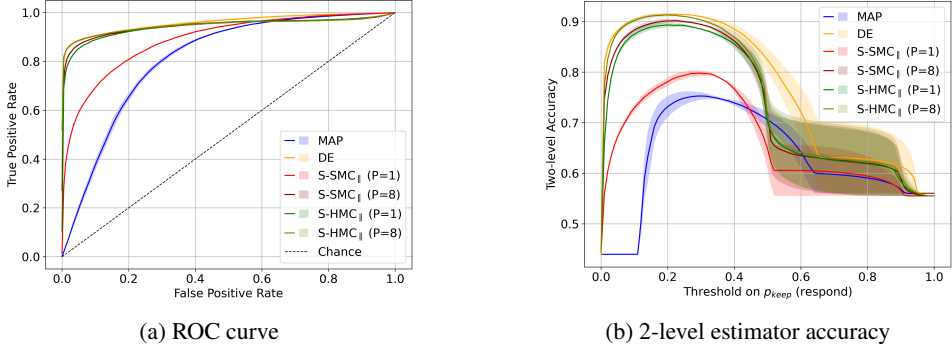


Figure 18: Averaged curve plots for OOD detection in IMDB. S-SMC_{||} ($P = 1, 8$ chain with $N = 10$), S-HMC_{||} (NP chains), DE (N models) and MAP, with fixed number of leapfrog $L = 1$, $B = 26$, $M = 2$, $v = 1$ and $s = 0.35$ (5 realizations and \pm s.e. in metrics).

G.3 CIFAR10

In the CIFAR10 case, the full setting is described in Appendix E.3.3, where we let $N_{\text{id}} = 9000$ and $N_{\text{ood}} = 9000$, and each dataset has 3000 data points. Metrics of Precision, Recall, F1 and AUC-ROC metrics are given in Table 7, the normalized confusion rate matrices to show how the OOD domain has been detected from the ID domain are given in Figure 19. Plots for ROC curve and 2-level estimator accuracy are given in Figure 20.

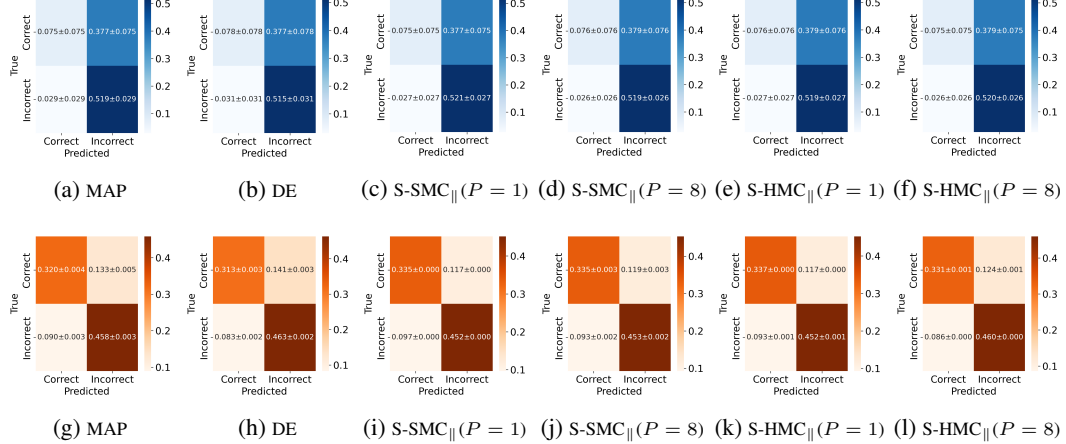
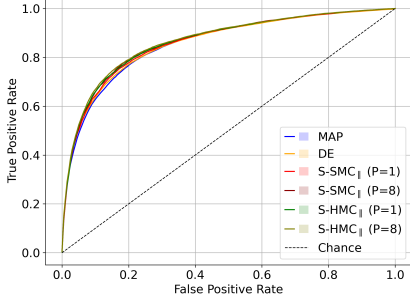


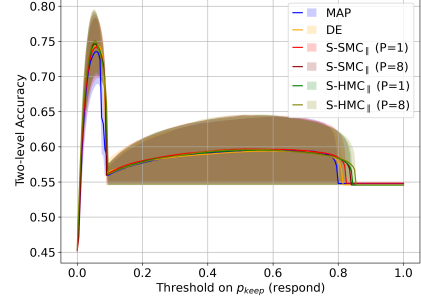
Figure 19: Averaged confusion rate matrices for OOD prediction on CIFAR10, with default decision threshold (top) and optimal F_1 decision threshold (bottom). S-SMC_{||} ($P = 1, 8$ chains with $N = 10$), S-HMC_{||} (NP chains), DE (N) and MAP, with fixed number of leapfrog $L = 1$, $B = 200$, $M = 4$, $v = 0.2$ and $s = 0.05$ (5 realizations and \pm s.e. in metrics).

Table 7: Evaluation Metrics using thresholds. S-SMC_{||} ($P = 1, 8$ chains with $N = 10$), S-HMC_{||} (NP chains), DE (N) and MAP, with fixed number of leapfrog $L = 1$, $B = 200$, $M = 4$, $v = 0.2$ and $s = 0.05$ (5 realizations, \pm s.e. in metrics and bold the first 30% data in mean).

P	Method	(a) Default decision threshold (0.5).				(b) Optimal F_1 decision threshold.			
		Precision	Recall	F1	AUC-ROC	Precision	Recall	F1	AUC-ROC
-	MAP	0.606 \pm 0.058	0.947 \pm 0.053	0.723 \pm 0.015	0.856 \pm 0.001	0.776 \pm 0.005	0.836 \pm 0.006	0.805 \pm 0.001	0.856 \pm 0.001
-	DE	0.608\pm0.062	0.943 \pm 0.057	0.721 \pm 0.015	0.858 \pm 0.002	0.767 \pm 0.003	0.848\pm0.003	0.805 \pm 0.001	0.858 \pm 0.002
1	S-SMC	0.607\pm0.059	0.951 \pm 0.049	0.726\pm0.018	0.861 \pm 0.001	0.794\pm0.000	0.824 \pm 0.001	0.809 \pm 0.000	0.861 \pm 0.001
8	S-SMC	0.606 \pm 0.060	0.952\pm0.048	0.725\pm0.019	0.864\pm0.000	0.792 \pm 0.003	0.830 \pm 0.003	0.811\pm0.000	0.864\pm0.000
1	S-HMC	0.606 \pm 0.060	0.951 \pm 0.049	0.724 \pm 0.019	0.864\pm0.000	0.794\pm0.000	0.829 \pm 0.001	0.811\pm0.000	0.864\pm0.000
8	S-HMC	0.605 \pm 0.060	0.953\pm0.047	0.725\pm0.019	0.867\pm0.000	0.788 \pm 0.001	0.842\pm0.001	0.814\pm0.000	0.867\pm0.000



(a) ROC curve



(b) Total accuracy over thresholds

Figure 20: Averaged curve plots for OOD detection in CIFAR10. S-SMC_{||} ($P = 1, 8$ chains with $N = 10$), S-HMC_{||} (NP chains), DE (N) and MAP, with fixed number of leapfrog $L = 1$, $B = 200$, $M = 4$, $v = 0.2$ and $s = 0.05$ (5 realizations and \pm s.e. in metrics).

H Further results of Ablations in Practical SBMC($s < \frac{1}{2}$)

H.1 MNIST7

Experiments in this section are tested on the (filtered) MNIST7 dataset with the model setting stated in Appendix E.3.1.

Table 8 shows the performance as the tuning parameter s varies. Figure 21 and 22 show the trend of the SBMC_{||} in different values of the tuning parameter s as P increases. Table 15 and 16 give the corresponding full data results of the below figures.

Table 8: Comparison of different s of (S-)SMC $_{\parallel}$ ($P = 1, 8$ chain with $N = 10$), (S-)HMC $_{\parallel}$ (NP chains), MAP and DE (NP models), with fixed number of leapfrog $L = 1$ and $v = 0.1$, on MNIST7 (5 realizations and \pm s.e. in accuracy).

s	Method	Epochs	Accuracy	NLLL	Brier	H_{ep}					
						ID		OD			
						cor.	inc.	8	9	wn	per.
1	HMC (GS)	2e4	93.61 \pm 0.41	2.224e-1	1.015e-1	9.621e-2	4.097e-1	4.614e-1	3.119e-1	1.126e+0	7.919e-1
	HMC (GS)	2e5	94.77 \pm 0.21	1.942e-1	8.700e-2	1.204e-1	4.928e-1	5.635e-1	4.067e-1	1.602e+0	1.031e+0
	HMC (GS)	1.8e6	95.13 \pm 0.02	1.882e-1	8.345e-2	1.281e-1	5.185e-1	5.856e-1	4.244e-1	1.682e+0	1.112e+0
1	SMC $_{\parallel}$	173.0	79.74 \pm 2.71	6.230e-1	2.920e-1	1.337e-2	3.339e-2	3.321e-2	2.775e-2	6.482e-2	5.512e-2
	HMC $_{\parallel}$	160	78.41 \pm 2.39	1.273e+0	5.799e-1	3.026e-1	3.247e-1	3.173e-1	2.988e-1	6.626e-1	1.099e+0
0.5	S-SMC $_{\parallel}$	161.0	84.18 \pm 0.64	4.827e-1	2.304e-1	1.556e-2	4.082e-2	4.000e-2	3.234e-2	1.238e-1	6.418e-2
	S-HMC $_{\parallel}$	160	85.26 \pm 1.06	8.234e-1	3.672e-1	2.993e-1	3.704e-1	3.627e-1	3.271e-1	8.832e-1	8.030e-1
0.25	S-SMC $_{\parallel}$	166.6	90.35 \pm 0.26	3.300e-1	1.441e-1	2.257e-2	1.094e-1	1.146e-1	7.791e-2	3.888e-1	1.996e-1
	$P = 8$	161.5	93.00 \pm 0.11	2.366e-1	1.096e-1	8.828e-2	3.717e-1	2.984e-1	2.089e-1	7.488e-1	4.585e-1
	S-HMC $_{\parallel}$	160	92.79 \pm 0.19	2.571e-1	1.156e-1	1.133e-1	4.232e-1	4.985e-1	3.225e-1	1.289e+0	6.280e-1
	$P = 8$	160	93.15 \pm 0.05	2.490e-1	1.127e-1	1.384e-1	4.788e-1	5.572e-1	3.678e-1	1.349e+0	7.311e-1
0.1	S-SMC $_{\parallel}$	170.0	92.17 \pm 0.37	2.671e-1	1.186e-1	2.642e-2	1.288e-1	1.384e-1	9.406e-2	3.943e-1	1.832e-1
	$P = 8$	178.0	93.26 \pm 0.16	2.259e-1	1.025e-1	5.871e-2	2.725e-1	2.440e-1	1.637e-1	7.238e-1	3.823e-1
	S-HMC $_{\parallel}$	160	92.96 \pm 0.17	2.326e-1	1.071e-1	5.624e-2	2.645e-1	3.072e-1	1.941e-1	9.304e-1	4.216e-1
	$P = 8$	160	93.12 \pm 0.08	2.310e-1	1.072e-1	6.982e-2	2.993e-1	3.524e-1	2.258e-1	1.067e+0	4.780e-1
0.01	S-SMC $_{\parallel}$	183.6	92.57 \pm 0.37	2.439e-1	1.121e-1	1.149e-2	5.904e-2	6.445e-2	4.602e-2	2.187e-1	1.008e-1
	S-HMC $_{\parallel}$	162	92.95 \pm 0.10	2.289e-1	1.069e-1	1.912e-2	1.015e-1	1.238e-1	7.814e-2	4.678e-1	1.945e-1
0	MAP	160.2	92.32 \pm 0.37	2.527e-1	1.163e-1	0	0	0	0	0	0
	DE (N)	176.5	92.40 \pm 0.15	2.455e-1	1.148e-1	1.059e-2	5.646e-2	7.433e-2	3.468e-2	2.690e-1	1.1056e-1
	DE ($8N$)	178.38	92.54 \pm 0.06	2.393e-1	1.124e-1	1.111e-2	5.980e-2	7.846e-2	4.016e-2	2.935e-1	1.188e-1

s	Method	H_{tot}					
		ID		OD			
		cor.	inc.	8	9	wn	per.
1	HMC (GS)	2.621e-1	9.652e-1	1.110e+0	8.198e-1	1.492e+0	1.081e+0
	HMC (GS)	2.852e-1	1.033e+0	1.204e+0	9.322e-1	1.915e+0	1.296e+0
	HMC (GS)	2.948e-1	1.057e+0	1.223e+0	9.532e-1	2.012e+0	1.384e+0
1	SMC $_{\parallel}$	5.506e-1	1.078e+0	1.138e+0	9.851e-1	6.426e-1	9.171e-1
	HMC $_{\parallel}$	1.854e+0	1.962e+0	1.988e+0	1.927e+0	1.965e+0	1.844e+0
0.5	S-SMC $_{\parallel}$	4.363e-1	1.019e+0	1.127e+0	9.294e-1	8.128e-1	8.712e-1
	S-HMC $_{\parallel}$	1.427e+0	1.752e+0	1.837e+0	1.667e+0	1.857e+0	1.694e+0
0.25	S-SMC $_{\parallel}$	1.508e-1	6.679e-1	8.384e-1	5.945e-1	8.495e-1	7.445e-1
	$P = 8$	1.247e-1	6.641e-1	1.000e+0	7.354e-1	1.177e+0	9.931e-1
	S-HMC $_{\parallel}$	3.149e-1	1.026e+0	1.220e+0	8.606e-1	1.624e+0	1.019e+0
	$P = 8$	3.456e-1	1.070e+0	1.267e+0	9.025e-1	1.714e+0	1.111e+0
0.1	S-SMC $_{\parallel}$	1.536e-1	7.042e-1	8.975e-1	6.591e-1	9.743e-1	8.001e-1
	$P = 8$	1.374e-1	7.075e-1	1.001e+0	7.307e-1	1.216e+0	9.805e-1
	S-HMC $_{\parallel}$	2.343e-1	9.132e-1	1.091e+0	7.567e-1	1.452e+0	8.443e-1
	$P = 8$	2.553e-1	9.380e-1	1.127e+0	7.893e-1	1.543e+0	8.937e-1
0.01	S-SMC $_{\parallel}$	1.737e-1	7.571e-1	9.632e-1	6.607e-1	9.254e-1	8.511e-1
	S-HMC $_{\parallel}$	1.995e-1	8.232e-1	1.003e+0	6.991e-1	1.234e+0	6.726e-1
0	MAP	1.833e-1	7.645e-1	9.507e-1	6.157e-1	7.682e-1	7.839e-1
	DE (N)	1.919e-1	7.899e-1	9.821e-1	6.393e-1	9.806e-1	8.112e-1
	DE ($8N$)	1.938e-1	7.988e-1	1.001e+0	6.532e-1	1.067e+0	8.133e-1

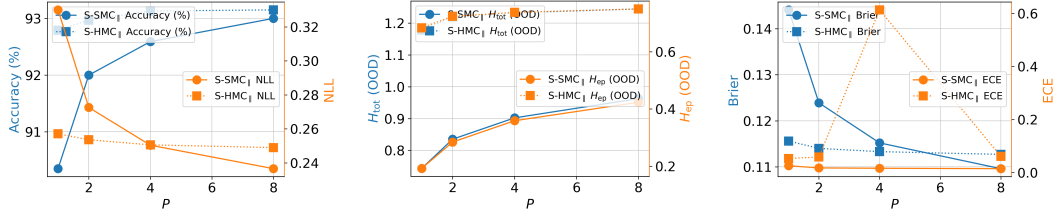


Figure 21: Comparison of S-SMC_{||} (P chains with $N = 10$) and S-HMC_{||} (NP chains), with fixed number of leapfrog $L = 1$, $B = 160$, $M = 7$, $v = 0.1$ and $s = 0.25$, on MNIST7 (5 realizations).

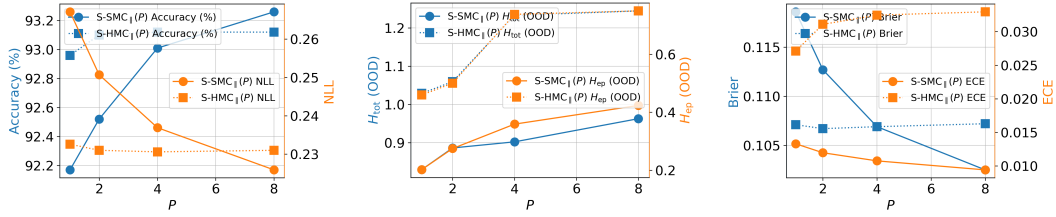


Figure 22: Comparison of S-SMC_{||} (P chains with $N = 10$) and S-HMC_{||} (NP chains), with fixed number of leapfrog $L = 1$, $B = 160$, $M = 10$, $v = 0.1$ and $s = 0.1$, on MNIST7 (5 realizations).

H.2 IMDB

The experiments in this section are tested on the IMDb dataset with the model setting stated in Appendix E.3.2.

Experiment with ($v = \frac{1}{40}$). Summary metrics of IMDb dataset with $v = 0.025$ and $s = 0.1$ is shown in the left spider-plot in Figure 3. Table 9 shows the performance as the tuning parameter s varies. Figure 23 shows the trend for the SBMC methods as P increases, where the full data can be found in Table 17.

Table 9: Comparison of S-SMC_{||} ($N = 10$), S-HMC_{||} (N chains), DE (N models) and MAP, with fixed number of leapfrog $L = 1$, $B = 25$, $M = 1$ and $v = 0.025$, on IMDb (5 realizations and \pm s.e. in accuracy).

s	Method	Ep.	Acc.	NL	H _{ep}							
					ID				OD			
					cor.	inc.	reviews	meta	lipsum	full reviews	full meta	
0.1	S-SMC	18.60	86.70 \pm 0.03	3.655e-1	1.122e-4	1.664e-4	1.792e-4	2.200e-4	1.749e-4	3.285e-4	3.212e-4	
	$P = 8$	19.15	86.69 \pm 0.01	3.653e-1	2.531e-4	3.697e-4	4.744e-4	4.971e-4	4.862e-4	5.876e-4	6.105e-4	
	S-HMC	25	86.70 \pm 0.01	3.634e-1	2.418e-4	3.565e-4	4.598e-4	4.633e-4	4.260e-4	5.057e-4	5.410e-4	
	$P = 8$	25	86.72 \pm 0.00	3.633e-1	2.766e-4	4.022e-4	5.694e-4	6.062e-4	5.637e-4	7.438e-4	7.051e-4	
0	MAP	25.00	84.47 \pm 0.09	3.911e-1	0	0	0	0	0	0	0	
	DE (N)	25.86	84.76 \pm 0.08	3.888e-1	1.005e-04	1.366e-04	5.064e-5	5.026e-5	4.909e-5	6.302e-5	5.548e-5	

s	Method	Brier	ECE	H _{tot}							
				ID				OD			
				cor.	inc.	reviews	meta	lipsum	full reviews	full meta	
0.1	S-SMC	1.093e-1	3.699e-1	4.792e-1	6.357e-1	5.251e-1	5.463e-1	5.142e-1	6.457e-1	6.261e-1	
	$P = 8$	1.092e-1	3.698e-1	4.788e-1	6.355e-1	5.213e-1	5.406e-1	5.115e-1	6.430e-1	6.236e-1	
	S-HMC	1.086e-1	3.694e-1	4.750e-1	6.340e-1	5.165e-1	5.331e-1	5.079e-1	6.400e-1	6.180e-1	
	$P = 8$	1.086e-1	3.701e-1	4.752e-1	6.341e-1	5.184e-1	5.359e-1	5.085e-1	6.426e-1	6.209e-1	
0	MAP	1.204e-1	4.389e-1	4.800e-1	6.306e-1	5.814e-1	6.117e-1	5.894e-1	6.705e-1	6.658e-1	
	DE (N)	1.193e-1	4.340e-1	4.819e-1	6.319e-1	5.793e-1	6.098e-1	5.882e-1	6.702e-1	6.649e-1	

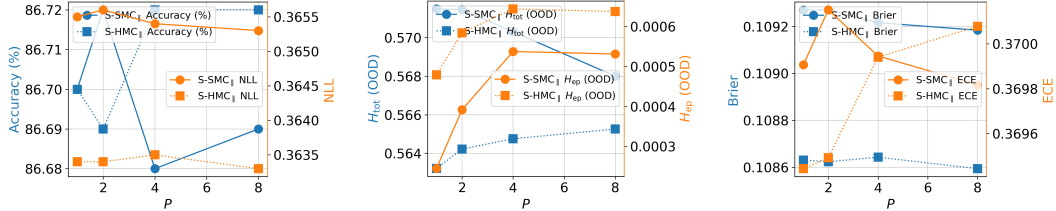


Figure 23: Comparison of S-SMC_{||} (P chains with $N = 10$) and S-HMC_{||} (NP chains), with fixed $L = 1$, $B = 25$, $M = 1$, $v = 0.025$, $s = 0.1$, on IMDb (5 realizations)

Experiments with $v = 1$. Summary metrics of IMDb dataset with $v = 15$ and $s = 0.35$ are shown in the spider-plot in Figure 24. Table 10 shows the performance as the tuning parameter s vary. Figure 25, 26 and 27 give the full convergence of SBMC_{||} with increasing P . The corresponding full data results are given in the Table 18, 19 and 20.

Table 10: Comparison of different s of S-SMC_{||} ($N = 10$) and S-HMC_{||} (N chains), with fixed number of leapfrog $L = 1$ and $v = 1$, on IMDb (5 realizations and \pm s.e. in accuracy).

s	Method	Ep.	Acc.	NL	H _{ep}							
					ID				OD			
					cor.	inc.	reviews	meta	lipsum	full reviews	full meta	
0.35	S-SMC $P = 8$	27.40	88.27 \pm 0.07	2.803e-1	6.177e-4	1.460e-3	1.581e-3	2.495e-3	2.187e-3	2.279e-3	2.504e-3	
		27.63	88.88 \pm 0.03	2.714e-1	9.342e-3	2.164e-2	3.756e-2	5.515e-2	5.260e-2	6.049e-2	6.435e-2	
	S-HMC $P = 8$	26	88.81 \pm 0.01	2.750e-1	1.565e-2	3.463e-2	5.414e-2	7.021e-2	6.872e-2	8.407e-2	7.930e-2	
		26	88.93 \pm 0.02	2.737e-1	1.662e-2	3.651e-2	5.315e-2	7.391e-2	6.917e-2	9.098e-2	8.360e-2	
0.25	S-SMC $P = 8$	29.6	88.27 \pm 0.10	2.807e-1	2.512e-4	6.069e-4	4.733e-4	7.166e-4	8.590e-4	9.313e-4	9.520e-4	
		28.5	88.87 \pm 0.03	2.720e-1	8.124e-3	1.872e-2	3.066e-2	5.057e-2	4.691e-2	6.403e-2	5.777e-2	
	S-HMC $P = 8$	26	88.83 \pm 0.02	2.745e-1	1.269e-2	2.830e-2	4.522e-2	5.927e-2	5.886e-2	7.342e-2	6.803e-2	
		26	88.92 \pm 0.02	2.734e-1	1.337e-2	2.964e-2	4.442e-2	6.215e-2	5.863e-2	7.869e-2	7.108e-2	
0.1	S-SMC $P = 8$	24	88.54 \pm 0.11	2.762e-1	1.820e-4	4.315e-4	4.819e-4	5.915e-4	6.766e-4	7.711e-4	6.500e-4	
		23.7	88.92 \pm 0.01	2.711e-1	4.207e-3	9.768e-3	2.182e-2	3.140e-2	2.700e-2	3.352e-2	3.540e-2	
	S-HMC $P = 8$	26	88.86 \pm 0.02	2.726e-1	5.753e-3	1.319e-2	2.712e-2	3.551e-2	3.561e-2	5.110e-2	4.289e-2	
		26	88.93 \pm 0.01	2.721e-1	6.065e-3	1.386e-2	2.792e-2	3.888e-2	3.653e-2	5.408e-2	4.638e-2	
0	MAP	52	87.97 \pm 0.04	2.854e-1	—	0	0	0	0	0	0	
	DE (N)	26.52	87.75 \pm 0.02	2.921e-1	3.144e-3	7.055e-3	4.514e-2	5.054e-2	5.386e-2	7.963e-2	5.318e-2	
	DE ($8N$)	25.86	87.70 \pm 0.01	2.925e-1	3.469e-3	7.608e-3	4.394e-2	5.622e-2	5.089e-2	7.435e-2	6.198e-2	

s	Method	Brier	ECE		H _{tot}							
					ID				OD			
					cor.	inc.	reviews	meta	lipsum	full reviews	full meta	
0.35	S-SMC $P = 8$	8.547e-2	3.832e-1	2.643e-1	5.482e-1	3.802e-1	5.116e-1	5.172e-1	5.581e-1	5.286e-1		
		8.206e-2	3.899e-1	2.744e-1	5.596e-1	3.987e-1	5.555e-1	5.304e-1	6.025e-1	5.920e-1		
	S-HMC $P = 8$	8.298e-2	3.889e-1	2.890e-1	5.681e-1	4.289e-1	5.583e-1	5.556e-1	6.133e-1	6.120e-1		
		8.254e-2	3.904e-1	2.893e-1	5.683e-1	4.188e-1	5.626e-1	5.386e-1	6.156e-1	6.088e-1		
0.25	S-SMC $P = 8$	8.548e-2	3.825e-1	2.673e-1	5.500e-1	3.562e-1	4.872e-1	4.727e-1	5.548e-1	5.609e-1		
		8.220e-2	3.901e-1	2.772e-1	5.609e-1	3.891e-1	5.447e-1	5.340e-1	6.036e-1	5.874e-1		
	S-HMC $P = 8$	8.286e-2	3.896e-1	2.873e-1	5.667e-1	4.239e-1	5.585e-1	5.533e-1	6.117e-1	6.076e-1		
		8.249e-2	3.904e-1	2.871e-1	5.665e-1	4.138e-1	5.595e-1	5.338e-1	6.135e-1	6.047e-1		
0.1	S-SMC $P = 8$	8.387e-2	3.869e-1	2.721e-1	5.544e-1	3.970e-1	5.202e-1	5.063e-1	5.686e-1	5.684e-1		
		8.190e-2	3.906e-1	2.752e-1	5.588e-1	3.920e-1	5.407e-1	5.143e-1	5.959e-1	5.865e-1		
	S-HMC $P = 8$	8.232e-2	3.898e-1	2.802e-1	5.618e-1	4.088e-1	5.505e-1	5.384e-1	6.066e-1	5.975e-1		
		8.217e-2	3.906e-1	2.801e-1	5.613e-1	4.028e-1	5.510e-1	5.231e-1	6.081e-1	5.961e-1		
0	MAP	8.714e-2	4.350e-1	2.721e-1	5.531e-1	4.071e-1	5.598e-1	5.462e-1	5.695e-1	5.561e-1		
	DE (N)	8.928e-2	4.343e-1	2.850e-1	5.580e-1	4.497e-1	5.808e-1	5.609e-1	6.185e-1	6.032e-1		
	DE ($8N$)	8.941e-2	4.354e-1	2.859e-1	5.588e-1	4.533e-1	5.888e-1	5.708e-1	6.187e-1	6.068e-1		

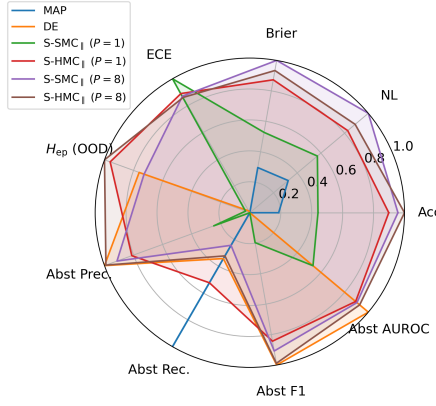


Figure 24: Summary metrics for IMDb in all methods. $S\text{-SMC}_{\parallel}$ ($P = 1$ chain with $N = 10$), $S\text{-HMC}_{\parallel}$ (NP chains), DE (N models) and MAP, with fixed number of leapfrog $L = 1$, $B = 26$, $M = 2$, $v = 1$ and $s = 0.35$ (5 realizations).

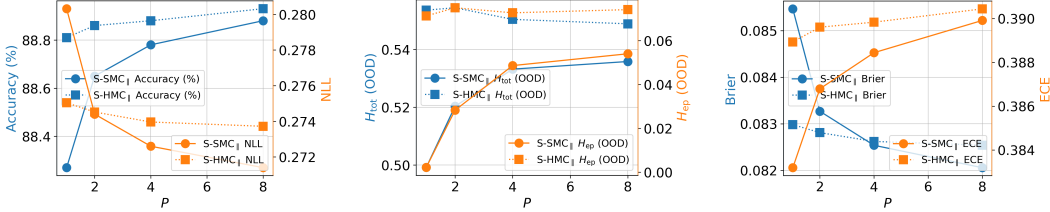


Figure 25: Comparison of $S\text{-SMC}_{\parallel}$ (P chains with $N = 10$) and $S\text{-HMC}_{\parallel}$ (NP chains), with fixed number of leapfrog $L = 1$, $B = 26$, $M = 1$, $v = 1$ and $s = 0.35$, on IMDb (5 realizations and \pm s.e. in accuracy).

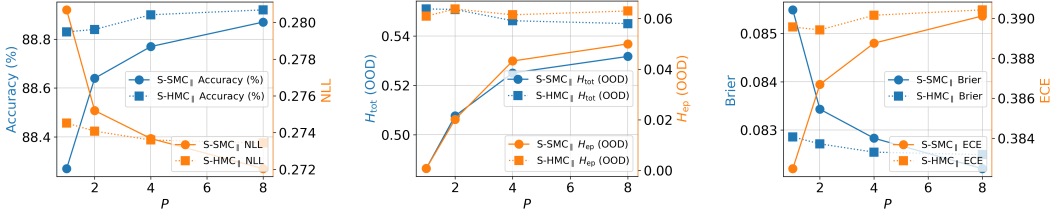


Figure 26: Comparison of $S\text{-SMC}_{\parallel}$ (P chains with $N = 10$) and $S\text{-HMC}_{\parallel}$ (NP chains), with fixed number of leapfrog $L = 1$, $B = 26$, $M = 2$, $v = 1$ and $s = 0.25$, on IMDb (5 realizations and \pm s.e. in accuracy).

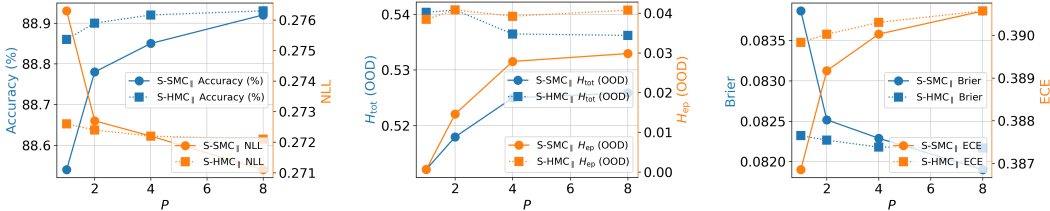


Figure 27: Comparison of $S\text{-SMC}_{\parallel}$ (P chains with $N = 10$) and $S\text{-HMC}_{\parallel}$ (NP chains), with fixed number of leapfrog $L = 1$, $B = 26$, $M = 2$, $v = 1$ and $s = 0.1$, on IMDb (5 realizations).

H.3 CIFAR10

Experiments in this section are tested on the CIFAR10 dataset with the model setting stated in Appendix E.3.3.

The summary metrics on CIFAR10 are shown in a spider-plot in Figure 3. Table 11 shows the performance as the tuning parameter s vary. Figure 28, 29 and 30 give the full convergence of SBMC_{\parallel} with increasing P . The corresponding full data results are given in Table 21, 22 and 23.

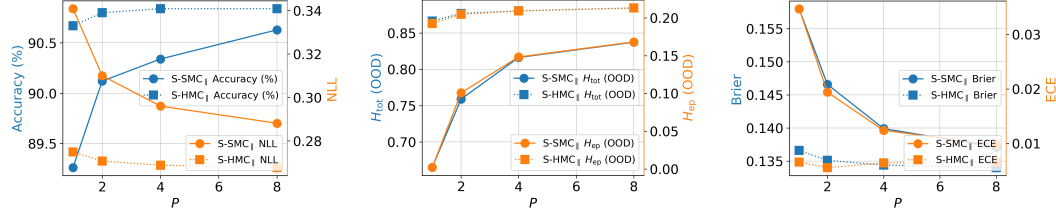


Figure 28: Comparison of S-SMC_{\parallel} (P chains with $N = 10$) and S-HMC_{\parallel} (NP chains), with fixed number of leapfrog $L = 1$, $B = 200$, $M = 4$, $v = 0.2$ and $s = 0.05$, on CIFAR10 (5 realizations).

Table 11: Comparison of S-SMC_{\parallel} ($N = 10$), S-HMC_{\parallel} (N chains), DE (N) and MAP, with fixed number of leapfrog $L = 1$, $B = 200$, $M = 4$ and $v = 0.2$, on CIFAR10 (5 realizations and \pm s.e. in accuracy).

s	Method	Ep.	Acc.	NL	Brier	ECE
0.2	S-SMC_{\parallel}	289.6	86.99 ± 0.08	$4.710\text{e-}1$	$2.007\text{e-}1$	$6.462\text{e-}2$
	$P = 8$	289.3	90.30 ± 0.03	$3.217\text{e-}1$	$1.445\text{e-}1$	$1.180\text{e-}2$
	S-HMC_{\parallel}	200	90.23 ± 0.08	$2.990\text{e-}1$	$1.466\text{e-}1$	$2.518\text{e-}2$
	$P = 8$	200	90.82 ± 0.03	$2.810\text{e-}1$	$1.395\text{e-}1$	$3.481\text{e-}2$
0.1	S-SMC_{\parallel}	229.6	88.26 ± 0.07	$3.855\text{e-}1$	$1.770\text{e-}1$	$4.593\text{e-}2$
	$P = 8$	225.3	90.45 ± 0.06	$2.980\text{e-}1$	$1.400\text{e-}1$	$7.737\text{e-}3$
	S-HMC_{\parallel}	200	90.57 ± 0.04	$2.823\text{e-}1$	$1.398\text{e-}1$	$1.073\text{e-}2$
	$P = 8$	200	90.83 ± 0.03	$2.701\text{e-}1$	$1.353\text{e-}1$	$1.517\text{e-}2$
0.05	S-SMC_{\parallel}	168.8	89.26 ± 0.07	$3.408\text{e-}1$	$1.580\text{e-}1$	$3.470\text{e-}2$
	$P = 8$	174.3	90.63 ± 0.05	$2.881\text{e-}1$	$1.371\text{e-}1$	$9.720\text{e-}3$
	S-HMC_{\parallel}	200	90.67 ± 0.03	$2.749\text{e-}1$	$1.366\text{e-}1$	$6.598\text{e-}3$
	$P = 8$	200	90.84 ± 0.03	$2.677\text{e-}1$	$1.340\text{e-}1$	$6.601\text{e-}3$
0	MAP	200	90.39 ± 0.07	$2.913\text{e-}1$	$1.420\text{e-}1$	$2.502\text{e-}2$
	DE (N)	200	90.81 ± 0.03	$2.741\text{e-}1$	$1.355\text{e-}1$	$1.770\text{e-}2$

s	Method	H_{ep}				H_{tot}					
		ID		OOD		ID		OOD			
		cor.	inc.	close	corrupt	far	cor.	inc.	close		
0.2	S-SMC_{\parallel}	$3.682\text{e-}4$	$1.947\text{e-}3$	$2.063\text{e-}3$	$1.092\text{e-}3$	$1.629\text{e-}3$	$1.136\text{e-}1$	$5.613\text{e-}1$	$5.440\text{e-}1$	$3.630\text{e-}1$	$7.756\text{e-}1$
	$P = 8$	$8.362\text{e-}2$	$3.326\text{e-}1$	$4.244\text{e-}1$	$2.361\text{e-}1$	$4.065\text{e-}1$	$1.071\text{e-}1$	$5.954\text{e-}1$	$9.675\text{e-}1$	$6.080\text{e-}1$	$1.160\text{e+}0$
	S-HMC_{\parallel}	$1.159\text{e-}1$	$4.091\text{e-}1$	$5.195\text{e-}1$	$2.993\text{e-}1$	$5.333\text{e-}1$	$2.676\text{e-}1$	$9.231\text{e-}1$	$1.059\text{e+}0$	$6.768\text{e-}1$	$1.297\text{e+}0$
	$P = 8$	$1.405\text{e-}1$	$4.604\text{e-}1$	$6.042\text{e-}1$	$3.476\text{e-}1$	$6.129\text{e-}1$	$2.945\text{e-}1$	$9.687\text{e-}1$	$1.146\text{e+}0$	$7.256\text{e-}1$	$1.364\text{e+}0$
0.1	S-SMC_{\parallel}	$2.948\text{e-}4$	$1.507\text{e-}3$	$1.603\text{e-}3$	$8.256\text{e-}4$	$1.450\text{e-}3$	$1.309\text{e-}1$	$6.364\text{e-}1$	$6.121\text{e-}1$	$4.027\text{e-}1$	$9.110\text{e-}1$
	$P = 8$	$5.539\text{e-}2$	$2.369\text{e-}1$	$3.054\text{e-}1$	$1.636\text{e-}1$	$2.937\text{e-}1$	$1.217\text{e-}1$	$6.453\text{e-}1$	$9.184\text{e-}1$	$5.690\text{e-}1$	$1.156\text{e+}0$
	S-HMC_{\parallel}	$7.055\text{e-}2$	$2.795\text{e-}1$	$3.591\text{e-}1$	$1.972\text{e-}1$	$3.581\text{e-}1$	$2.241\text{e-}1$	$8.596\text{e-}1$	$9.703\text{e-}1$	$6.102\text{e-}1$	$1.219\text{e+}0$
	$P = 8$	$1.035\text{e-}1$	$3.121\text{e-}1$	$4.095\text{e-}1$	$2.244\text{e-}1$	$4.031\text{e-}1$	$2.367\text{e-}1$	$8.884\text{e-}1$	$1.023\text{e+}0$	$6.371\text{e-}1$	$1.257\text{e+}0$
0.05	S-SMC_{\parallel}	$4.258\text{e-}4$	$2.273\text{e-}3$	$2.515\text{e-}3$	$1.297\text{e-}3$	$2.185\text{e-}3$	$1.351\text{e-}1$	$6.620\text{e-}1$	$6.639\text{e-}1$	$4.300\text{e-}1$	$9.008\text{e-}1$
	$P = 8$	$3.507\text{e-}2$	$1.584\text{e-}1$	$2.027\text{e-}1$	$1.058\text{e-}1$	$1.961\text{e-}1$	$1.311\text{e-}1$	$6.684\text{e-}1$	$8.643\text{e-}1$	$5.368\text{e-}1$	$1.111\text{e+}0$
	S-HMC_{\parallel}	$4.060\text{e-}2$	$1.804\text{e-}1$	$2.308\text{e-}1$	$1.228\text{e-}1$	$2.243\text{e-}1$	$1.917\text{e-}1$	$8.073\text{e-}1$	$8.900\text{e-}1$	$5.558\text{e-}1$	$1.154\text{e+}0$
	$P = 8$	$4.579\text{e-}2$	$1.966\text{e-}1$	$2.564\text{e-}1$	$1.358\text{e-}1$	$2.472\text{e-}1$	$1.971\text{e-}1$	$8.203\text{e-}1$	$9.173\text{e-}1$	$5.684\text{e-}1$	$1.168\text{e+}0$
0	MAP	0	0	0	0	0	$1.423\text{e-}1$	$7.037\text{e-}1$	$7.258\text{e-}1$	$4.577\text{e-}1$	$1.065\text{e+}0$
	DE (N)	$9.291\text{e-}3$	$4.753\text{e-}2$	$4.861\text{e-}2$	$2.603\text{e-}2$	$3.930\text{e-}2$	$1.541\text{e-}1$	$7.275\text{e-}1$	$7.629\text{e-}1$	$4.786\text{e-}1$	$1.029\text{e+}0$

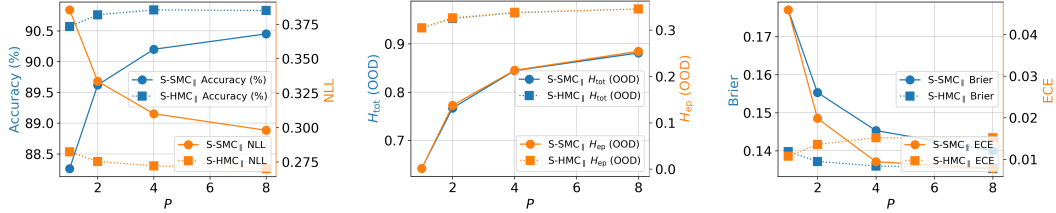


Figure 29: Comparison of S-SMC_{||} (P chains with $N = 10$) and S-HMC_{||} (NP chains), with fixed number of leapfrog $L = 1$, $B = 200$, $M = 4$, $v = 0.2$ and $s = 0.1$, on CIFAR10 (5 realizations).

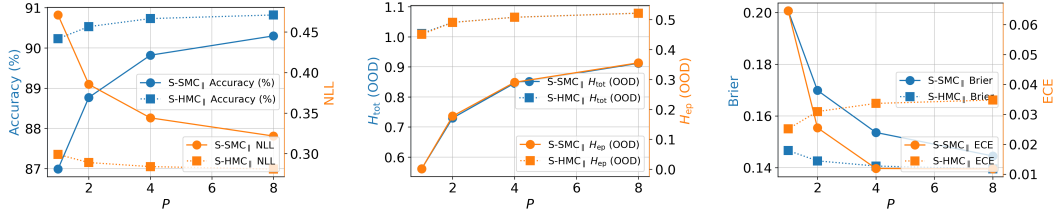


Figure 30: Comparison of S-SMC_{||} (P chains with $N = 10$) and S-HMC_{||} (NP chains), with fixed number of leapfrog $L = 1$, $B = 200$, $M = 4$, $v = 0.2$ and $s = 0.2$, on CIFAR10 (5 realizations).

I All-inclusive data tables

Table 12: Comparison in all domains among S-SMC_{||} ($P = 1$ chain with $N = 10$), S-HMC_{||} (NP chains), HMC (GS) (2e4 samples), DE (N models) and MAP, with fixed number of leapfrog $L = 1$, $v = 0.1$ and $s = 0.1$, on MNIST7 (5 realizations and \pm s.e. in entropy).

Group	MAP			DE			S-HMC ($s = 0.1$)			S-SMC ($s = 0.1$)			HMC (GS) ($s = 1$)		
	H_{tot}	H_{tot}	H_{al}	H_{tot}	H_{al}	H_{ep}	H_{tot}	H_{al}	H_{ep}	H_{tot}	H_{al}	H_{ep}	H_{tot}	H_{al}	H_{ep}
Digit 0	1.276e-1	1.307e-1	1.237e-1	7.076e-3	1.671e-1	1.228e-1	4.427e-2	1.110e-1	8.528e-2	2.574e-2	2.157e-1	1.268e-1	8.893e-2		
Digit 1	1.768e-1	1.840e-1	1.781e-1	5.823e-3	1.889e-1	1.585e-1	3.038e-2	1.408e-1	1.255e-1	1.535e-2	2.124e-1	1.621e-1	5.025e-2		
Digit 2	2.294e-1	2.266e-1	2.142e-1	1.236e-2	2.980e-1	2.168e-1	8.122e-2	2.090e-1	1.679e-1	4.118e-2	3.410e-1	1.988e-1	1.423e-1		
Digit 3	3.168e-1	3.493e-1	3.222e-1	2.711e-2	3.883e-1	2.896e-1	9.873e-2	2.686e-1	2.245e-1	4.404e-2	4.229e-1	2.616e-1	1.613e-1		
Digit 4	2.158e-1	2.221e-1	2.103e-1	1.182e-2	2.753e-1	2.095e-1	6.583e-2	1.981e-1	1.654e-1	3.272e-2	2.925e-1	1.847e-1	1.078e-1		
Digit 5	3.993e-1	4.058e-1	3.787e-1	2.712e-2	4.395e-1	3.224e-1	1.171e-1	3.056e-1	2.520e-1	5.366e-2	4.428e-1	2.655e-1	1.773e-1		
Digit 6	1.856e-1	2.045e-1	1.927e-1	1.180e-2	2.836e-1	2.047e-1	7.891e-2	1.856e-1	1.495e-1	3.605e-2	2.968e-1	1.785e-1	1.182e-1		
Digit 7	1.897e-1	1.957e-1	1.859e-1	9.730e-3	2.403e-1	1.802e-1	6.008e-2	1.693e-1	1.396e-1	2.967e-2	2.528e-1	1.569e-1	9.589e-2		
Digit 8	9.507e-1	9.821e-1	9.078e-1	7.433e-2	1.091e+0	7.836e-1	3.072e-1	8.975e-1	7.591e-1	1.384e-1	1.121e+0	6.333e-1	4.873e-1		
Digit 9	6.157e-1	6.393e-1	6.046e-1	3.468e-2	7.567e-1	5.626e-1	1.941e-1	6.591e-1	5.651e-1	9.406e-2	9.210e-1	5.554e-1	3.657e-1		
Perturbed	7.528e-1	8.112e-1	7.006e-1	1.106e-1	8.443e-1	4.227e-1	4.216e-1	8.001e-1	6.169e-1	1.832e-1	1.228e+0	2.819e-1	9.466e-1		
White Noise	7.703e-1	9.806e-1	7.117e-1	2.690e-1	1.453e+0	5.221e-1	9.304e-1	9.744e-1	5.800e-1	3.944e-1	1.398e+0	3.444e-1	1.053e+0		
All ID	2.301e-1	2.398e-1	2.069e-1	3.291e-2	2.821e-1	2.111e-1	7.090e-2	1.966e-1	1.623e-1	3.429e-2	1.021e+0	5.943e-1	4.265e-1		

Table 13: Comparison in all domains among S-SMC $_{\parallel}$ ($P = 1$ chain with $N = 10$), S-HMC $_{\parallel}$ (NP chains), DE (N models) and MAP, with fixed number of leapfrog $L = 1$, $B = 25$, $M = 1$, $v = 0.025$ and $s = 0.1$, on IMDb (5 realizations).

Group	MAP		DE				S-HMC $_{\parallel}$			S-SMC $_{\parallel}$		
	H_{tot}	H_{tot}	H_{al}	H_{ep}	H_{tot}	H_{al}	H_{ep}	H_{tot}	H_{al}	H_{ep}		
Negative	4.352e-1	4.407e-1	4.406e-1	9.314e-5	4.892e-1	4.889e-1	2.482e-4	4.929e-1	4.927e-1	1.148e-4		
Positive	5.716e-1	5.688e-1	5.687e-1	1.188e-4	5.031e-1	5.029e-1	2.659e-4	5.072e-1	5.071e-1	1.240e-4		
Meta	6.117e-1	6.098e-1	6.097e-1	5.026e-5	5.331e-1	5.326e-1	4.633e-4	5.463e-1	5.461e-1	2.200e-4		
Full Meta	6.658e-1	6.649e-1	6.649e-1	5.548e-5	6.185e-1	6.180e-1	5.410e-4	6.260e-1	6.257e-1	3.212e-4		
Reviews	5.814e-1	5.793e-1	5.793e-1	5.064e-5	5.165e-1	5.160e-1	4.598e-4	5.251e-1	5.249e-1	1.792e-4		
Full reviews	6.705e-1	6.702e-1	6.701e-1	6.302e-5	6.400e-1	6.395e-1	5.057e-4	6.457e-1	6.454e-1	3.285e-4		
Lipsum	5.894e-1	5.882e-1	5.881e-1	4.909e-5	5.079e-1	5.074e-1	4.260e-4	5.142e-1	5.140e-1	1.749e-4		
All ID	5.034e-1	5.048e-1	5.046e-1	1.060e-4	4.962e-1	4.959e-1	2.570e-4	5.000e-1	4.999e-1	1.194e-4		

Table 14: Comparison in all domains among S-SMC $_{\parallel}$ ($P = 8$ chain with $N = 10$), S-HMC $_{\parallel}$ (NP chains), DE (N models) and MAP, with fixed number of leapfrog $L = 1$, $B = 26$, $M = 2$, $v = 1$ and $s = 0.35$, on IMDb (5 realizations).

Group	MAP		DE				S-HMC $_{\parallel}$			S-SMC $_{\parallel}$		
	H_{tot}	H_{tot}	H_{al}	H_{ep}	H_{tot}	H_{al}	H_{ep}	H_{tot}	H_{al}	H_{ep}		
Negative	2.489e-1	2.494e-1	2.483e-1	1.033e-3	3.107e-1	2.928e-1	1.794e-2	2.962e-1	2.860e-1	1.016e-2		
Positive	3.629e-1	3.675e-1	3.659e-1	1.631e-3	3.296e-1	3.099e-1	1.971e-2	3.160e-1	3.048e-1	1.126e-2		
Meta	5.598e-1	5.767e-1	5.507e-1	2.594e-2	5.626e-1	4.887e-1	7.391e-2	5.555e-1	5.004e-1	5.514e-2		
Full Meta	5.561e-1	5.737e-1	5.469e-1	2.683e-2	6.088e-1	5.251e-1	8.360e-2	5.920e-1	5.277e-1	6.435e-2		
Reviews	4.071e-1	4.251e-1	4.030e-1	2.212e-2	4.188e-1	3.657e-1	5.315e-2	3.987e-1	3.611e-1	3.756e-2		
Full reviews	5.695e-1	6.007e-1	5.574e-1	4.331e-2	6.156e-1	5.246e-1	9.098e-2	6.025e-1	5.420e-1	6.049e-2		
Lipsum	5.462e-1	5.556e-1	5.283e-1	2.733e-2	5.386e-1	4.695e-1	6.917e-2	5.304e-1	4.778e-1	5.260e-2		
All ID	3.059e-1	3.084e-1	3.071e-1	1.332e-3	3.202e-1	3.013e-1	1.883e-2	3.061e-1	2.954e-1	1.071e-2		

Table 17: Comparison of S-SMC $_{\parallel}$ (P chains with $N = 10$) and S-HMC $_{\parallel}$ (NP chains), with fixed $L = 1$, $B = 25$, $M = 1$, $v = 0.025$, $s = 0.1$, on IMDb (5 realizations and \pm s.e. in accuracy).

P	Method	Ep.	Acc.	NL	H_{ep}								
					ID		OOD						
					cor.	inc.	reviews	meta	lipsum	full reviews	full meta		
1	S-SMC $_{\parallel}$	18.60	86.70 \pm 0.03	3.655e-1	1.122e-4	1.664e-4	1.792e-4	2.200e-4	1.749e-4	3.285e-4	3.212e-4		
	S-HMC $_{\parallel}$	25	86.70 \pm 0.01	3.634e-1	2.418e-4	3.565e-4	4.598e-4	4.633e-4	4.260e-4	5.057e-4	5.410e-4		
2	S-SMC $_{\parallel}$	18.70	86.72 \pm 0.03	3.656e-1	1.936e-4	2.798e-4	3.061e-4	3.358e-4	4.211e-4	4.491e-4	4.465e-4		
	S-HMC $_{\parallel}$	25	86.69 \pm 0.01	3.634e-1	2.697e-4	3.955e-4	5.604e-4	5.852e-4	4.916e-4	6.022e-4	6.819e-4		
4	S-SMC $_{\parallel}$	19.10	86.68 \pm 0.02	3.654e-1	2.370e-4	3.452e-4	4.433e-4	4.874e-4	5.515e-4	5.848e-4	6.201e-4		
	S-HMC $_{\parallel}$	25	86.72 \pm 0.01	3.635e-1	2.776e-4	4.042e-4	5.940e-4	6.264e-4	5.629e-4	7.074e-4	7.288e-4		
8	S-SMC $_{\parallel}$	19.15	86.69 \pm 0.01	3.653e-1	2.531e-4	3.697e-4	4.744e-4	4.971e-4	4.862e-4	5.876e-4	6.105e-4		
	S-HMC $_{\parallel}$	25	86.72 \pm 0.00	3.633e-1	2.766e-4	4.022e-4	5.694e-4	6.062e-4	5.637e-4	7.438e-4	7.051e-4		
P	Method	Brier	ECE	H_{tot}									
				ID		OOD							
				cor.	inc.	reviews	meta	lipsum	full reviews	full meta			
1	S-SMC $_{\parallel}$	1.093e-1	3.699e-1	4.792e-1	6.357e-1	5.251e-1	5.463e-1	5.142e-1	6.457e-1	6.261e-1			
	S-HMC $_{\parallel}$	1.086e-1	3.694e-1	4.750e-1	6.340e-1	5.165e-1	5.331e-1	5.079e-1	6.400e-1	6.186e-1			
2	S-SMC $_{\parallel}$	1.093e-1	3.702e-1	4.793e-1	6.356e-1	5.243e-1	5.466e-1	5.131e-1	6.462e-1	6.270e-1			
	S-HMC $_{\parallel}$	1.086e-1	3.695e-1	4.752e-1	6.342e-1	5.172e-1	5.342e-1	5.092e-1	6.409e-1	6.196e-1			
4	S-SMC $_{\parallel}$	1.092e-1	3.699e-1	4.787e-1	6.355e-1	5.230e-1	5.440e-1	5.127e-1	6.459e-1	6.259e-1			
	S-HMC $_{\parallel}$	1.086e-1	3.699e-1	4.754e-1	6.342e-1	5.180e-1	5.351e-1	5.085e-1	6.419e-1	6.203e-1			
8	S-SMC $_{\parallel}$	1.092e-1	3.698e-1	4.788e-1	6.355e-1	5.213e-1	5.406e-1	5.115e-1	6.430e-1	6.236e-1			
	S-HMC $_{\parallel}$	1.086e-1	3.701e-1	4.752e-1	6.341e-1	5.184e-1	5.359e-1	5.085e-1	6.426e-1	6.209e-1			

Table 15: Comparison of S-SMC $_{\parallel}$ (P chains with $N = 10$) and S-HMC $_{\parallel}$ (NP chains), with fixed number of leapfrog $L = 1$, $B = 160$, $M = 7$, $v = 0.1$ and $s = 0.25$, on MNIST7 (5 realizations and \pm s.e. in accuracy).

P	Method	Ep.	Acc.	NL	Brier
1	S-SMC $_{\parallel}$	166.6	90.35 \pm 0.26	3.300e-1	1.441e-1
	S-HMC $_{\parallel}$	160	92.79 \pm 0.19	2.571e-1	1.156e-1
2	S-SMC $_{\parallel}$	160.3	92.00 \pm 0.24	2.726e-1	1.239e-1
	S-HMC $_{\parallel}$	160	92.97 \pm 0.14	2.536e-1	1.140e-1
4	S-SMC $_{\parallel}$	164.5	92.59 \pm 0.15	2.504e-1	1.152e-1
	S-HMC $_{\parallel}$	160	93.13 \pm 0.07	2.506e-1	1.133e-1
8	S-SMC $_{\parallel}$	161.5	93.00 \pm 0.11	2.366e-1	1.096e-1
	S-HMC $_{\parallel}$	160	93.15 \pm 0.05	2.490e-1	1.127e-1
HMC (GS)		2e4	92.87 \pm 0.48	2.376e-1	1.079e-1

P	Method	H_{ep}						H_{tot}					
		ID			OOD			ID			OOD		
		cor.	inc.	8	9	wn	per.	cor.	inc.	8	9	wn	per.
1	S-SMC $_{\parallel}$	2.257e-2	1.094e-1	1.146e-1	7.791e-2	3.847e-1	1.914e-1	1.508e-1	6.679e-1	8.384e-1	5.945e-1	8.290e-1	7.110e-1
	S-HMC $_{\parallel}$	1.133e-1	4.232e-1	4.985e-1	3.225e-1	1.281e+0	6.314e-1	3.149e-1	1.026e+0	1.220e+0	8.606e-1	1.614e+0	1.019e+0
2	S-SMC $_{\parallel}$	5.445e-2	2.442e-1	1.975e-1	1.402e-1	5.073e-1	2.923e-1	1.371e-1	6.768e-1	9.108e-1	6.629e-1	9.559e-1	8.111e-1
	HMC $_{\parallel}$	1.298e-1	4.568e-1	5.380e-1	3.638e-1	1.321e+0	6.720e-1	3.358e-1	1.050e+0	1.250e+0	8.975e-1	1.680e+0	1.050e+0
4	S-SMC $_{\parallel}$	7.492e-2	3.240e-1	2.544e-1	1.797e-1	6.264e-1	3.749e-1	1.287e-1	6.669e-1	9.591e-1	7.064e-1	1.051e+0	8.923e-1
	HMC $_{\parallel}$	1.356e-1	4.718e-1	5.508e-1	3.634e-1	1.327e+0	7.084e-1	3.443e-1	1.065e+0	1.261e+0	9.031e-1	1.689e+0	1.078e+0
8	S-SMC $_{\parallel}$	8.828e-2	3.717e-1	2.984e-1	2.089e-1	7.384e-1	4.475e-1	1.247e-1	6.641e-1	1.001e+0	7.354e-1	1.152e+0	9.627e-1
	S-HMC $_{\parallel}$	1.384e-1	4.788e-1	5.572e-1	3.678e-1	1.349e+0	7.235e-1	3.456e-1	1.070e+0	1.267e+0	9.025e-1	1.715e+0	1.094e+0
HMC (GS)		7.199e-2	3.432e-1	3.887e-1	2.748e-1	1.169e+0	5.579e-1	2.045e-1	8.566e-1	9.984e-1	7.425e-1	1.574e+0	8.725e-1

Table 20: Comparison of S-SMC $_{\parallel}$ (P chains with $N = 10$) and S-HMC $_{\parallel}$ (NP chains), with fixed number of leapfrog $L = 1$, $B = 26$, $M = 2$, $v = 1$ and $s = 0.1$, on IMDb (5 realizations and \pm s.e. in accuracy).

P	Method	Ep.	Acc.	NL	H_{ep}								
					ID				OOD				
					cor.	inc.	reviews	meta	lipsum	full reviews	full meta		
1	S-SMC $_{\parallel}$	24	88.54 \pm 0.11	2.763e-1	1.820e-4	4.315e-4	4.819e-4	5.915e-4	6.766e-4	7.711e-4	6.500e-4		
	S-HMC $_{\parallel}$	26	88.86 \pm 0.02	2.726e-1	5.753e-3	1.319e-2	2.712e-2	3.551e-2	3.561e-2	5.110e-2	4.289e-2		
2	S-SMC $_{\parallel}$	23.2	88.78 \pm 0.08	2.727e-1	2.476e-3	5.724e-3	1.160e-2	1.973e-2	9.401e-3	1.314e-2	1.894e-2		
	S-HMC $_{\parallel}$	26	88.90 \pm 0.02	2.724e-1	5.934e-3	1.365e-2	2.817e-2	3.918e-2	3.793e-2	5.296e-2	4.581e-2		
4	S-SMC $_{\parallel}$	23.5	88.85 \pm 0.05	2.722e-1	3.730e-3	8.583e-3	1.937e-2	2.851e-2	2.377e-2	3.216e-2	3.538e-2		
	S-HMC $_{\parallel}$	26	88.92 \pm 0.01	2.722e-1	5.992e-3	1.368e-2	2.753e-2	3.839e-2	3.531e-2	5.049e-2	4.444e-2		
8	S-SMC $_{\parallel}$	23.7	88.92 \pm 0.01	2.711e-1	4.207e-3	9.768e-3	2.182e-2	3.140e-2	2.700e-2	3.352e-2	3.540e-2		
	S-HMC $_{\parallel}$	26	88.93 \pm 0.01	2.721e-1	6.065e-3	1.386e-2	2.792e-2	3.888e-2	3.653e-2	5.408e-2	4.638e-2		

P	Method	Brier	ECE	H_{tot}								
				ID				OOD				
				cor.	inc.	reviews	meta	lipsum	full reviews	full meta		
1	S-SMC $_{\parallel}$	8.387e-2	3.869e-1	2.721e-1	5.544e-1	3.970e-1	5.202e-1	5.063e-1	5.686e-1	5.684e-1		
	S-HMC $_{\parallel}$	8.232e-2	3.898e-1	2.802e-1	5.618e-1	4.088e-1	5.505e-1	5.384e-1	6.066e-1	5.975e-1		
2	S-SMC $_{\parallel}$	8.252e-2	3.892e-1	2.734e-1	5.571e-1	3.939e-1	5.263e-1	5.028e-1	5.812e-1	5.855e-1		
	S-HMC $_{\parallel}$	8.227e-2	3.900e-1	2.801e-1	5.614e-1	4.092e-1	5.567e-1	5.347e-1	6.068e-1	5.966e-1		
4	S-SMC $_{\parallel}$	8.229e-2	3.900e-1	2.750e-1	5.583e-1	3.944e-1	5.389e-1	5.114e-1	5.948e-1	5.854e-1		
	S-HMC $_{\parallel}$	8.218e-2	3.903e-1	2.800e-1	5.612e-1	4.041e-1	5.526e-1	5.222e-1	6.068e-1	5.967e-1		
8	S-SMC $_{\parallel}$	8.190e-2	3.906e-1	2.752e-1	5.588e-1	3.920e-1	5.407e-1	5.143e-1	5.959e-1	5.865e-1		
	S-HMC $_{\parallel}$	8.217e-2	3.906e-1	2.801e-1	5.613e-1	4.028e-1	5.510e-1	5.231e-1	6.081e-1	5.961e-1		

Table 16: Comparison of S-SMC $_{\parallel}$ (P chains with $N = 10$) and S-HMC $_{\parallel}$ (NP chains), with fixed number of leapfrog $L = 1$, $B = 160$, $M = 10$, $v = 0.1$ and $s = 0.1$, on MNIST7 (5 realizations and \pm s.e. in accuracy).

P	Method	Ep.	Acc.	NL	Brier
1	S-SMC $_{\parallel}$	170.0	92.17 \pm 0.37	2.671e-1	1.186e-1
	S-HMC $_{\parallel}$	160	92.96 \pm 0.17	2.326e-1	1.071e-1
2	S-SMC $_{\parallel}$	179.0	92.52 \pm 0.30	2.507e-1	1.127e-1
	S-HMC $_{\parallel}$	160	93.10 \pm 0.12	2.310e-1	1.067e-1
4	S-SMC $_{\parallel}$	180.5	93.01 \pm 0.29	2.369e-1	1.069e-1
	HMC $_{\parallel}$	160	93.12 \pm 0.09	2.306e-1	1.069e-1
8	S-SMC $_{\parallel}$	178.0	93.26 \pm 0.16	2.259e-1	1.025e-1
	S-HMC $_{\parallel}$	160	93.12 \pm 0.09	2.310e-1	1.072e-1
HMC (GS)		2e4	92.92 \pm 0.41	2.366e-1	1.084e-1

P	Method	H_{ep}						H_{tot}					
		ID			OOD			ID			OOD		
		cor.	inc.	8	9	wn	per.	cor.	inc.	8	9	wn	per.
1	S-SMC $_{\parallel}$	2.642e-2	1.288e-1	1.384e-1	9.406e-2	3.972e-1	1.776e-1	1.536e-1	7.042e-1	8.975e-1	6.591e-1	9.753e-1	7.859e-1
	S-HMC $_{\parallel}$	5.624e-2	2.645e-1	3.072e-1	1.941e-1	9.259e-1	4.100e-1	2.343e-1	9.132e-1	1.091e+0	7.567e-1	1.443e+0	8.248e-1
2	S-SMC $_{\parallel}$	4.233e-2	2.042e-1	1.836e-1	1.227e-1	5.306e-1	2.620e-1	1.449e-1	7.053e-1	9.422e-1	6.870e-1	1.058e+0	8.577e-1
	S-HMC $_{\parallel}$	6.494e-2	2.844e-1	3.395e-1	2.198e-1	9.977e-1	4.432e-1	2.472e-1	9.223e-1	1.112e+0	7.769e-1	1.506e+0	8.436e-1
4	S-SMC $_{\parallel}$	5.315e-2	2.471e-1	2.200e-1	1.465e-1	6.363e-1	3.288e-1	1.403e-1	7.019e-1	9.791e-1	7.130e-1	1.126e+0	9.159e-1
	S-HMC $_{\parallel}$	6.733e-2	2.924e-1	3.479e-1	2.179e-1	1.010e+0	4.740e-1	2.520e-1	9.300e-1	1.119e+0	7.823e-1	1.493e+0	8.866e-1
8	S-SMC $_{\parallel}$	5.872e-2	2.725e-1	2.440e-1	1.637e-1	7.309e-1	3.750e-1	1.374e-1	7.075e-1	1.001e+0	7.307e-1	1.220e+0	9.649e-1
	S-HMC $_{\parallel}$	6.982e-2	2.993e-1	3.524e-1	2.258e-1	1.066e+0	4.817e-1	2.553e-1	9.380e-1	1.127e+0	7.893e-1	1.539e+0	8.946e-1
HMC (GS)		5.034e-2	2.417e-1	2.713e-1	1.900e-1	9.303e-1	3.683e-1	2.076e-1	8.477e-1	1.001e+0	7.264e-1	1.430e+0	7.518e-1

Table 18: Comparison of S-SMC $_{\parallel}$ (P chains with $N = 10$) and S-HMC $_{\parallel}$ (NP chains), with fixed number of leapfrog $L = 1$, $B = 26$, $M = 1$, $v = 1$ and $s = 0.35$, on IMDb (5 realizations and \pm s.e. in accuracy).

P	Method	Ep.	Acc.	NL	H_{ep}								
					ID				OOD				
					cor.	inc.	reviews	meta	lipsum	full reviews	full meta		
1	S-SMC $_{\parallel}$	27.40	88.27 \pm 0.07	2.803e-1	6.177e-4	1.460e-3	1.581e-3	2.495e-3	2.187e-3	2.279e-3	2.504e-3		
	S-HMC $_{\parallel}$	26.00	88.81 \pm 0.01	2.750e-1	1.565e-2	3.463e-2	5.414e-2	7.021e-2	6.872e-2	8.407e-2	7.930e-2		
2	S-SMC $_{\parallel}$	27.70	88.65 \pm 0.04	2.744e-1	5.513e-3	1.323e-2	2.132e-2	3.443e-2	2.751e-2	2.232e-2	3.585e-2		
	S-HMC $_{\parallel}$	26.00	88.86 \pm 0.03	2.745e-1	1.620e-2	3.584e-2	5.510e-2	7.622e-2	7.118e-2	8.766e-2	8.490e-2		
4	S-SMC $_{\parallel}$	28.55	88.78 \pm 0.03	2.726e-1	8.040e-3	1.881e-2	3.057e-2	4.854e-2	5.097e-2	5.547e-2	5.766e-2		
	S-HMC $_{\parallel}$	26.00	88.88 \pm 0.01	2.740e-1	1.640e-2	3.610e-2	5.388e-2	7.488e-2	6.705e-2	8.588e-2	8.184e-2		
8	S-SMC $_{\parallel}$	27.63	88.88 \pm 0.03	2.714e-1	9.342e-3	2.164e-2	3.756e-2	5.515e-2	5.260e-2	6.049e-2	6.435e-2		
	S-HMC $_{\parallel}$	26.00	88.93 \pm 0.02	2.737e-1	1.662e-2	3.651e-2	5.315e-2	7.391e-2	6.917e-2	9.098e-2	8.360e-2		

P	Method	Brier	ECE	H_{tot}								
				ID				OOD				
				cor.	inc.	reviews	meta	lipsum	full reviews	full meta		
1	S-SMC $_{\parallel}$	8.547e-2	3.832e-1	2.643e-1	5.482e-1	3.802e-1	5.116e-1	5.172e-1	5.581e-1	5.286e-1		
	S-HMC $_{\parallel}$	8.298e-2	3.889e-1	2.890e-1	5.681e-1	4.289e-1	5.583e-1	5.556e-1	6.133e-1	6.120e-1		
2	S-SMC $_{\parallel}$	8.327e-2	3.868e-1	2.694e-1	5.548e-1	3.937e-1	5.456e-1	5.091e-1	5.790e-1	5.742e-1		
	S-HMC $_{\parallel}$	8.281e-2	3.896e-1	2.891e-1	5.681e-1	4.285e-1	5.684e-1	5.521e-1	6.125e-1	6.107e-1		
4	S-SMC $_{\parallel}$	8.254e-2	3.884e-1	2.720e-1	5.576e-1	3.985e-1	5.601e-1	5.295e-1	5.963e-1	5.815e-1		
	S-HMC $_{\parallel}$	8.262e-2	3.898e-1	2.891e-1	5.684e-1	4.232e-1	5.673e-1	5.377e-1	6.139e-1	6.100e-1		
8	S-SMC $_{\parallel}$	8.206e-2	3.899e-1	2.744e-1	5.596e-1	3.987e-1	5.555e-1	5.304e-1	6.025e-1	5.920e-1		
	S-HMC $_{\parallel}$	8.254e-2	3.904e-1	2.893e-1	5.683e-1	4.188e-1	5.626e-1	5.386e-1	6.156e-1	6.088e-1		

Table 19: Comparison of S-SMC $_{\parallel}$ (P chains with $N = 10$) and S-HMC $_{\parallel}$ (NP chains), with fixed number of leapfrog $L = 1$, $B = 26$, $M = 2$, $v = 1$ and $s = 0.25$, on IMDb (5 realizations and \pm s.e. in accuracy).

P	Method	Ep.	Acc.	NL	H_{ep}								
					ID				OOD				
					cor.	inc.	reviews	meta	lipsum	full reviews	full meta		
1	S-SMC $_{\parallel}$	29.6	88.27 \pm 0.10	2.807e-1	2.512e-4	6.069e-4	4.733e-4	7.166e-4	8.590e-4	9.313e-4	9.520e-4		
	S-HMC $_{\parallel}$	26	88.83 \pm 0.02	2.745e-1	1.269e-2	2.830e-2	4.522e-2	5.927e-2	5.886e-2	7.342e-2	6.803e-2		
2	S-SMC $_{\parallel}$	27.2	88.64 \pm 0.05	2.752e-1	4.948e-3	1.174e-2	1.344e-2	2.120e-2	1.410e-2	2.411e-2	2.792e-2		
	S-HMC $_{\parallel}$	26	88.84 \pm 0.03	2.741e-1	1.304e-2	2.918e-2	4.586e-2	6.400e-2	6.096e-2	7.596e-2	7.216e-2		
4	S-SMC $_{\parallel}$	28.3	88.77 \pm 0.04	2.737e-1	7.211e-3	1.662e-2	2.329e-2	4.029e-2	4.913e-2	5.544e-2	4.798e-2		
	S-HMC $_{\parallel}$	26	88.90 \pm 0.1	2.736e-1	1.321e-2	2.932e-2	4.487e-2	6.264e-2	5.689e-2	7.369e-2	6.930e-2		
8	S-SMC $_{\parallel}$	28.5	88.87 \pm 0.03	2.720e-1	8.124e-3	1.872e-2	3.066e-2	5.057e-2	4.691e-2	6.403e-2	5.777e-2		
	S-HMC $_{\parallel}$	26	88.92 \pm 0.02	2.734e-1	1.337e-2	2.964e-2	4.442e-2	6.215e-2	5.863e-2	7.869e-2	7.108e-2		

P	Method	Brier	ECE	H_{tot}							
				ID				OOD			
				cor.	inc.	reviews	meta	lipsum	full reviews	full meta	
1	S-SMC $_{\parallel}$	8.548e-2	3.825e-1	2.673e-1	5.500e-1	3.562e-1	4.872e-1	4.727e-1	5.548e-1	5.609e-1	
	S-HMC $_{\parallel}$	8.286e-2	3.896e-1	2.873e-1	5.667e-1	4.239e-1	5.585e-1	5.533e-1	6.117e-1	6.076e-1	
2	S-SMC $_{\parallel}$	8.343e-2	3.867e-1	2.723e-1	5.560e-1	3.696e-1	5.182e-1	4.861e-1	5.794e-1	5.849e-1	
	S-HMC $_{\parallel}$	8.271e-2	3.894e-1	2.870e-1	5.668e-1	4.228e-1	5.661e-1	5.478e-1	6.112e-1	6.061e-1	
4	S-SMC $_{\parallel}$	8.283e-2	3.888e-1	2.758e-1	5.589e-1	3.823e-1	5.388e-1	5.321e-1	5.920e-1	5.801e-1	
	S-HMC $_{\parallel}$	8.254e-2	3.902e-1	2.870e-1	5.665e-1	4.174e-1	5.633e-1	5.328e-1	6.118e-1	6.058e-1	
8	S-SMC $_{\parallel}$	8.220e-2	3.901e-1	2.772e-1	5.609e-1	3.891e-1	5.447e-1	5.340e-1	6.036e-1	5.874e-1	
	S-HMC $_{\parallel}$	8.249e-2	3.904e-1	2.871e-1	5.665e-1	4.138e-1	5.595e-1	5.338e-1	6.135e-1	6.047e-1	

Table 21: Comparison of S-SMC $_{\parallel}$ (P chains with $N = 10$) and S-HMC $_{\parallel}$ (NP chains), with fixed number of leapfrog $L = 1$, $B = 200$, $M = 4$, $v = 0.2$ and $s = 0.05$, on CIFAR10 (5 realizations and \pm s.e. in accuracy).

P	Method	Ep.	Acc.	NL	H_{ep}		H_{tot}						
					ID		OOD				ID		
					cor.	inc.	close	corrupt	far	cor.	inc.	close	corrupt
1	S-SMC $_{\parallel}$	4.258e-4	2.273e-3	2.515e-3	1.297e-3	2.185e-3	1.351e-1	6.620e-1	6.639e-1	4.300e-1	9.008e-1		
	S-HMC $_{\parallel}$	4.060e-2	1.804e-1	2.308e-1	1.228e-1	2.243e-1	1.917e-1	8.073e-1	8.900e-1	5.558e-1	1.154e+0		
2	S-SMC $_{\parallel}$	1.796e-2	9.094e-2	1.115e-1	5.702e-2	1.340e-1	1.321e-1	6.646e-1	7.737e-1	4.864e-1	1.017e+0		
	S-HMC $_{\parallel}$	4.376e-2	1.896e-1	2.454e-1	1.300e-1	2.387e-1	1.956e-1	8.144e-1	9.064e-1	5.626e-1	1.162e+0		
4	S-SMC $_{\parallel}$	2.855e-2	1.356e-1	1.700e-1	8.859e-2	1.862e-1	1.304e-1	6.700e-1	8.293e-1	5.188e-1	1.101e+0		
	S-HMC $_{\parallel}$	4.523e-2	1.937e-1	2.520e-1	1.337e-1	2.417e-1	1.970e-1	8.161e-1	9.129e-1	5.660e-1	1.163e+0		
8	S-SMC $_{\parallel}$	3.507e-2	1.584e-1	2.027e-1	1.058e-1	1.961e-1	1.311e-1	6.684e-1	8.643e-1	5.368e-1	1.111e+0		
	S-HMC $_{\parallel}$	4.579e-2	1.966e-1	2.564e-1	1.358e-1	2.472e-1	1.971e-1	8.203e-1	9.173e-1	5.684e-1	1.168e+0		

Table 22: Comparison of S-SMC $_{\parallel}$ (P chains with $N = 10$) and S-HMC $_{\parallel}$ (NP chains), with fixed number of leapfrog $L = 1$, $B = 200$, $M = 4$, $v = 0.2$ and $s = 0.1$, on CIFAR10 (5 realizations and \pm s.e. in accuracy).

P	Method	Ep.	Acc.	NL	Brier	ECE
1	S-SMC $_{\parallel}$	229.6	88.26 ± 0.07	3.855e-1	1.770e-1	4.593e-2
1	S-HMC $_{\parallel}$	200	90.57 ± 0.04	2.823e-1	1.398e-1	1.073e-2
2	S-SMC $_{\parallel}$	226.0	89.62 ± 0.09	3.336e-1	1.553e-1	1.983e-2
2	S-HMC $_{\parallel}$	200	90.76 ± 0.04	2.753e-1	1.372e-1	1.356e-2
4	S-SMC $_{\parallel}$	224.8e	90.20 ± 0.08	3.100e-1	1.453e-1	9.413e-3
4	S-HMC $_{\parallel}$	200	90.84 ± 0.04	2.722e-1	1.360e-1	1.517e-2
8	S-SMC $_{\parallel}$	225.3	90.45 ± 0.06	2.980e-1	1.400e-1	7.737e-3
8	S-HMC $_{\parallel}$	200	90.83 ± 0.03	2.701e-1	1.353e-1	1.517e-2

P	Method	H_{ep}				H_{tot}					
		ID		OOD		ID		OOD			
		cor.	inc.	close	corrupt	far	cor.	inc.	close		
1	S-SMC $_{\parallel}$	2.948e-4	1.507e-3	1.603e-3	8.256e-4	1.450e-3	1.309e-1	6.364e-1	6.121e-1	4.027e-1	9.110e-1
1	S-HMC $_{\parallel}$	7.055e-2	2.795e-1	3.591e-1	1.972e-1	3.581e-1	2.241e-1	8.596e-1	9.703e-1	6.102e-1	1.219e+0
2	S-SMC $_{\parallel}$	2.733e-2	1.343e-1	1.594e-1	8.581e-2	1.677e-1	1.256e-1	6.382e-1	7.735e-1	4.910e-1	1.037e+0
2	S-HMC $_{\parallel}$	9.734e-2	2.968e-1	3.862e-1	2.112e-1	3.821e-1	2.316e-1	8.732e-1	9.990e-1	6.238e-1	1.235e+0
4	S-SMC $_{\parallel}$	4.484e-2	2.002e-1	2.495e-1	1.365e-1	2.536e-1	1.235e-1	6.432e-1	8.577e-1	5.408e-1	1.135e+0
4	S-HMC $_{\parallel}$	1.018e-1	3.072e-1	4.011e-1	2.200e-1	3.936e-1	2.360e-1	8.822e-1	1.014e+0	6.323e-1	1.247e+0
8	S-SMC $_{\parallel}$	5.539e-2	2.369e-1	3.054e-1	1.636e-1	2.937e-1	1.217e-1	6.453e-1	9.184e-1	5.690e-1	1.156e+0
8	S-HMC $_{\parallel}$	1.035e-1	3.121e-1	4.095e-1	2.244e-1	4.031e-1	2.367e-1	8.884e-1	1.023e+0	6.371e-1	1.257e+0

Table 23: Comparison of S-SMC $_{\parallel}$ (P chains with $N = 10$) and S-HMC $_{\parallel}$ (NP chains), with fixed number of leapfrog $L = 1$, $B = 200$, $M = 4$, $v = 0.2$ and $s = 0.2$, on CIFAR10 (5 realizations and \pm s.e. in accuracy).

P	Method	Ep.	Acc.	NL	Brier	ECE
1	S-SMC $_{\parallel}$	289.6	86.99 ± 0.08	4.710e-1	2.007e-1	6.462e-2
1	S-HMC $_{\parallel}$	200	90.23 ± 0.08	2.990e-1	1.466e-1	2.518e-2
2	S-SMC $_{\parallel}$	289.6	88.77 ± 0.07	3.854e-1	1.699e-1	2.554e-2
2	S-HMC $_{\parallel}$	200	90.53 ± 0.04	2.890e-1	1.426e-1	3.096e-2
4	S-SMC $_{\parallel}$	289.4	89.82 ± 0.04	3.441e-1	1.536e-1	1.193e-2
4	S-HMC $_{\parallel}$	200	90.73 ± 0.02	2.840e-1	1.406e-1	3.368e-2
8	S-SMC $_{\parallel}$	289.3	90.30 ± 0.03	3.217e-1	1.445e-1	1.180e-2
8	S-HMC $_{\parallel}$	200	90.82 ± 0.03	2.810e-1	1.395e-1	3.481e-2

P	Method	H_{ep}				H_{tot}					
		ID		OOD		ID		OOD			
		cor.	inc.	close	corrupt	far	cor.	inc.	close		
1	S-SMC $_{\parallel}$	3.682e-4	1.947e-3	2.063e-3	1.092e-3	1.629e-3	1.136e-1	5.613e-1	5.440e-1	3.630e-1	7.756e-1
1	S-HMC $_{\parallel}$	1.159e-1	4.091e-1	5.195e-1	2.993e-1	5.333e-1	2.676e-1	9.231e-1	1.059e+0	6.768e-1	1.297e+0
2	S-SMC $_{\parallel}$	3.863e-2	1.856e-1	2.117e-1	1.180e-1	2.030e-1	1.108e-1	5.822e-1	7.557e-1	4.901e-1	9.434e-1
2	S-HMC $_{\parallel}$	1.300e-1	4.377e-1	5.681e-1	3.260e-1	5.774e-1	2.836e-1	9.479e-1	1.109e+0	7.039e-1	1.331e+0
4	S-SMC $_{\parallel}$	6.722e-2	2.780e-1	3.470e-1	1.916e-1	3.332e-1	1.089e-1	5.885e-1	8.861e-1	5.634e-1	1.087e+0
4	S-HMC $_{\parallel}$	1.368e-1	4.524e-1	5.899e-1	3.392e-1	5.947e-1	2.909e-1	9.611e-1	1.132e+0	7.169e-1	1.346e+0
8	S-SMC $_{\parallel}$	8.362e-2	3.326e-1	4.244e-1	2.361e-1	4.065e-1	1.071e-1	5.954e-1	9.675e-1	6.080e-1	1.160e+0
8	S-HMC $_{\parallel}$	1.405e-1	4.604e-1	6.042e-1	3.476e-1	6.129e-1	2.945e-1	9.687e-1	1.146e+0	7.256e-1	1.364e+0